OPEN ACCESS
Fractals, Vol. 30, No. 8 (2022) 2240270 (25 pages)

DOI: 10.1142/S0218348X22402708

World Scientific
www.worldscientific.com

MEMORY EFFECT ANALYSIS USING PIECEWISE CUBIC B-SPLINE OF TIME FRACTIONAL DIFFUSION EQUATION

MADIHA SHAFIQ
Department of Mathematics, University of Sargodha, Sargodha, Pakistan
madihashafiq007@gmail.com

FARAH AINI ABDULLAH*
School of Mathematical Sciences
Universiti Sains Malaysia, 11800 Penang, Malaysia
farahaini@usm.my

MUHAMMAD ABBAS
Department of Mathematics, University of Sargodha, Sargodha, Pakistan
muhammad.abbas@uos.edu.pk

AHMED SM ALZAIDI
Department of Mathematics and Statistics, College of Science, Taif University
P.O. Box 11099, Taif 21944, Saudi Arabia
azaidi@tu.edu.sa

MUHAMMAD BILAL RIAZ
Institute of Applied Mathematics, Faculty of Applied Physics and Mathematics
Gdańsk University of Technology, 80-233 Gdańsk, Poland
muhammad.riaz@pg.edu.pl

*Corresponding author.

Received August 8, 2021
Accepted November 10, 2021
Published December 6, 2022

Abstract

The purpose of this work is to study the memory effect analysis of Caputo–Fabrizio time fractional diffusion equation by means of cubic B-spline functions. The Caputo–Fabrizio interpretation of fractional derivative involves a non-singular kernel that permits to describe some class of material heterogeneities and the effect of memory more effectively. The proposed numerical technique relies on finite difference approach and cubic B-spline functions for discretization along temporal and spatial grids, respectively. To ensure that the error does not amplify during computational process, stability analysis is performed. The described algorithm is second-order convergent along time and space directions. The computational competence of the scheme is tested through some numerical examples. The results reveal that the current scheme is reasonably efficient and reliable to be used for solving the subject problem.

Keywords: Diffusion Equation; Spline Interpolation; Caputo–Fabrizio Fractional Derivative; Cubic B-Spline Functions; Stability; Finite Difference Formulation; Convergence.

1. INTRODUCTION

The advent of fractional calculus is as old as that of its classical counterpart. However, in the last two decades, it has gained a remarkable research attraction as it can be applied for solving many physical and engineering problems.[1–3] The fractional order differential equations have the potential to describe the dynamic processes more efficiently as compared to classical ones. Numerous applications are found in biomedical engineering, electrochemistry, hydrology, finance, rheology, probability theory, optics, signal processing and other disciplines of science and technology.[4–12] Several interpretations for fractional order derivatives have been proposed and each one of them has its own advantages and disadvantages, the interested readers are referred to Refs. 13–18. In this paper, we explore the approximate solutions of the following time fractional diffusion equation (TFDE):

$$ {}_0^{CF}D_t^{\gamma} w(v,t) = \frac{\partial^2 w(v,t)}{\partial v^2} + q(v,t), \quad \gamma \in (0,1), \quad v \in [a,b], \quad t \in [t_0, T], \tag{1} $$

with initial condition

$$ w(v,t_0) = \psi(v) \tag{2} $$

and the end conditions

$$ w(a,t) = \phi_1(t), \quad w(b,t) = \phi_2(t), \tag{3} $$

where ${}_0^{CF}D_t^{\gamma} w(v,t)$ represents the Caputo–Fabrizio fractional derivative (CFFD), ϕ_1, ϕ_2, ψ, q are assumed to be continuous functions and γ denotes the fractional order of time derivative. The development of improved and reliable techniques for solving linear and nonlinear fractional diffusion models has always remained a hot area of research. The diffusion equation has been studied by various authors using the Caputo time fractional derivative instead of first-order time derivative. Zhuang and Liu[19] employed an implicit difference approximation for solving TFDE. An explicit difference-based algorithm has been presented by Murillo and Yuste[20] for solutions of the fractional diffusion and diffusion wave equations with Caputo fractional derivative (CFD). Sweilam *et al.*[21] proposed the Crank–Nicolson scheme for numerical solution of TFDE. Sun *et al.*[22] employed the semi systematic finite element scheme for solving a collection of TFDEs. Mustapha *et al.*[23] developed a discontinuous Petrov–Galerkin technique for approximate solutions of TFDEs. In Ref. 24, Esmaeili and Garrappa constructed a pseudo-spectral method for numerical outcomes of TFDE. Tuan *et al.*[25] studied the inverse problem for one-dimensional TFDE by means of a modified regularization scheme using the frequency domain.

Atangana and Alkahtani[26] presented the model using fractional derivative with non-singular kernel

of resistance, inductance and capacitance electrical circuit. Atangana and Araz[27] have presented new concept in calculus of piecewise derivative with classical and global derivatives as well as with singular and non-singular kernels using numerical algorithm based on the Newton polynomial for epidemiological, fractional orders and fractal dimensions problems. In Ref. 28, Atangana and Alqahtani developed a numerical approach for advection dispersion equation with time-space CFFD and studied its application to groundwater pollution equation. A differential equation involving CFFD and its application to mass-spring-damper system have been investigated by Al-Salti *et al.*[29] Goufo[30] established the model of Korteweg–de Vries–Burgers equation with CFFD. Mirza and Vieru[31] used the Fourier and Laplace transforms to obtain fundamental solutions for two-dimensional advection–diffusion equation in Caputo–Fabrizio sense. Liu *et al.*[32] developed and analyzed the quasi-linear time fractional parabolic equation with non-singular kernel using finite difference scheme. Kumar *et al.*[33] proposed an iterative method for numerical solution of modified Kawahara equation involving fractional operator with exponential kernel. Shaikh *et al.*[34] investigated the approximate solutions of Fitzhugh–Nagumo and Fisher equation involving CFFD using an iterative Laplace transform method.

In recent years, numerous numerical techniques based on B-spline interpolation have been presented by different authors for solving the fractional differential equations. In particular, the spline functions are found to be powerful tools in curve approximation due to their rich geometrical features. The authors in Refs. 35–37 employed cubic trigonometric B-spline technique for approximate solutions of time fractional sub-diffusion, diffusion-wave and Burgers' equations. Khalid *et al.*[38] presented a technique based on modified extended cubic B-spline (CBS) functions for Caputo time fractional diffusion-wave equation with damping and reaction terms. In Ref. 39, Mohyud-Din *et al.* assembled extended cubic B-splines to develop a difference scheme for approximate solutions of time fractional advection diffusion equation. Numerical outcomes of time fractional telegraph equation have been presented by Akram *et al.*[40] using an extended form of CBS functions. Khalid *et al.*[41] proposed the application of non-polynomial fifth degree spline functions for computational study of fourth-order fractional ordinary differential equations containing product terms. The authors in Refs. 42 and 43 propounded a computational scheme based on non-polynomial quintic spline for solving fourth-order time fractional sub-diffusion and super-diffusion equations.

In this paper, a computational method based on CBS functions has been proposed for approximate solutions of TFDE. The θ-weighted formulation is used to carry out the presented algorithm. This method relies on Caputo–Fabrizio derivative with finite difference scheme for temporal discretization and CBS functions for interpolation along spatial grid. The stability and convergence of current numerical approach have also been presented. To the best of the author's knowledge, the proposed algorithm for TFDE is novel and it has not been noted in literature yet.

This paper is based on following framework: Some definitions are given in Sec. 2. In Sec. 3, derivation of the numerical method based on CBS functions is presented. The stability of the algorithm is analyzed in Sec. 4. Section 5 describes the convergence analysis. To corroborate the efficiency and accuracy of the scheme, results of computational experiments are recorded in Sec. 6 and finally, the conclusion is presented in Sec. 7.

2. PRELIMINARIES

Definition 1 (Ref. 27). Let $u(t)$ and $f(t)$ be two continuous functions such that $f(t)$ is increasing and non-constant and $u(t)$ is differentiable, then a piecewise derivative in local way within the interval $[0, T]$ is

$$ {}_0^{PG}D_t u(t) = \begin{cases} \dfrac{du(t)}{dt} & \text{if } t \in [0, t_0], \\ D_f u(t) & \text{if } t \in [t_0, T], \end{cases} \tag{4} $$

where $\frac{du(t)}{dt}$ and $D_f u(t)$ represent the classical derivative on $0 \le t \le t_0$ and global derivative on $t_0 \le t \le T$, respectively.

Definition 2 (Ref. 27). The piecewise derivative with classical and exponential decay kernel is defined within the interval $[0, T]$ as

$$ {}_0^{PCF}D_t^{\gamma} u(t) = \begin{cases} u'(t) & \text{if } t \in [0, t_0], \\ {}_0^{CF}D_t^{\gamma} u(t) & \text{if } t \in [t_0, T] \end{cases} \tag{5} $$

and

$$ {}_0^{PCF}D_t^{\gamma} u(t) = \begin{cases} u'(t) & \text{if } t \in [0, t_0], \\ {}_0^{CFR}D_t^{\gamma} u(t) & \text{if } t \in [t_0, T], \end{cases} \tag{6} $$

where ${}_0^{PCF}D_t^{\gamma} u(t)$ represents classical derivative on $0 \le t \le t_0$ and CFFD on $t_0 \le t \le T$.

Definition 3 (Ref. 44). The CFFD $\frac{\partial^\gamma}{\partial t^\gamma} w(v,t)$ with non-singular kernel of order $\gamma \in (0,1)$ is defined as

$$
\begin{aligned}
{}_0^{CF}D_t^\gamma w(v,t) &= \frac{\partial^\gamma}{\partial t^\gamma} w(v,t) \\
&= \frac{R(\gamma)}{1-\gamma} \int_0^t \frac{\partial}{\partial \kappa} w(v,\kappa) \\
&\quad \times \exp\left[-\frac{\gamma}{1-\gamma}(t-\kappa)\right] d\kappa, \\
&\quad \gamma \in (0,1), \qquad (7)
\end{aligned}
$$

where the normalization function $R(\gamma)$ satisfying the condition $R(0) = R(1) = 1$.

Definition 4 (Ref. 45). Parseval's identity is defined as

$$
\sum_{m=-\infty}^{\infty} |\hat{y}(m)|^2 = \int_a^b |\tilde{y}(v)|^2 dv, \quad \tilde{y} \in L^2[a,b], \qquad (8)
$$

where $\hat{y}(m) = \int_a^b \tilde{y}(v) e^{2\pi i m v} dv$ is the Fourier transform for every integer m.

3. THE DERIVATION OF NUMERICAL METHOD

Let the time domain $[0,T]$ be divided into M equal subintervals of the length $\Delta t = \frac{T}{M}$ using the knots $0 = t_0 < t_1 < \cdots < t_M = T$, where $t_n = n\Delta t$, $n = 0, 1, \ldots, M$ and the spatial domain $[a,b]$ be divided into N subintervals of equal length $h = \frac{b-a}{N}$ using the knots $a = v_0 < v_1 < \cdots < v_N = b$, where $v_r = v_0 + rh$, $r = 0, 1, \ldots, N$. For $w(v,t)$, the CBS approximation $W(v,t)$ can be assumed as

$$
W(v,t) = \sum_{r=-1}^{N+1} \alpha_r(t) S_r(v), \qquad (9)
$$

where $\alpha_r(t)$, time-dependent control points, are to be computed and $S_r(v)$, the CBS functions, are described as[46]

$$
S_r(v) = \frac{1}{6h^3} \begin{cases} (v - v_{r-2})^3 & \text{if } v \in [v_{r-2}, v_{r-1}), \\ \varsigma & \text{if } v \in [v_{r-1}, v_r), \\ \chi & \text{if } v \in [v_r, v_{r+1}), \\ (v_{r+2} - v)^3 & \text{if } v \in [v_{r+1}, v_{r+2}), \\ 0 & \text{otherwise}, \end{cases} \qquad (10)
$$

where

$$
\begin{aligned}
\varsigma &= h^3 + 3h^2(v - v_{r-1}) + 3h(v - v_{r-1})^2 \\
&\quad - 3(v - v_{r-1})^3 \\
\chi &= h^3 + 3h^2(v_{r+1} - v) + 3h(v_{r+1} - v)^2 \\
&\quad - 3(v_{r+1} - v)^3.
\end{aligned}
$$

The CBS functions have a lot of geometrical properties such as symmetry, non-negativity, convex hull property, geometric invariability, local support and the partition of unity.[46] Moreover, $S_{-1}, S_0, \ldots, S_{N+1}$ have been composed in such a way that they can serve as basis for space interval $[a,b]$. The relations (9) and (10) provide the following approximations:

$$
\begin{cases}
(W)_r = \left(\frac{1}{6}\right)\alpha_{r-1} + \left(\frac{4}{6}\right)\alpha_r + \left(\frac{1}{6}\right)\alpha_{r+1}, \\
(W_v)_r = \left(\frac{1}{2h}\right)\alpha_{r+1} + \left(-\frac{1}{2h}\right)\alpha_{r-1}, \\
(W_{vv})_r = \left(\frac{1}{h^2}\right)\alpha_{r-1} + \left(-\frac{2}{h^2}\right)\alpha_r \\
\qquad\qquad + \left(\frac{1}{h^2}\right)\alpha_{r+1}.
\end{cases} \qquad (11)
$$

Substituting (9) into (1), we get

$$
\frac{\partial^\gamma W(v,t)}{\partial t^\gamma} = \frac{\partial^2 W(v,t)}{\partial v^2} + q(v,t). \qquad (12)
$$

The Caputo–Fabrizio fractional time derivative involved in (12) is discretized at $t = t_{n+1}$ as

$$
\begin{aligned}
\frac{\partial^\gamma}{\partial t^\gamma} W(v,t_{n+1}) &= \frac{1}{1-\gamma} \int_0^{t_{n+1}} \frac{\partial}{\partial \kappa} W(v,\kappa) \\
&\quad \times \exp\left[-\frac{\gamma}{1-\gamma}(t_{n+1} - \kappa)\right] d\kappa, \\
&= \frac{1}{1-\gamma} \sum_{z=0}^{n} \int_{t_z}^{t_{z+1}} \frac{\partial}{\partial \kappa} W(v,\kappa) \\
&\quad \times \exp\left[-\frac{\gamma}{1-\gamma}(t_{n+1} - \kappa)\right] d\kappa. \qquad (13)
\end{aligned}
$$

Through forward difference formulation, equation (13) is modified as

$$
\begin{aligned}
&\frac{\partial^\gamma}{\partial t^\gamma} W(v,t_{n+1}) \\
&\quad = \frac{1}{1-\gamma} \sum_{z=0}^{n} \frac{W(v,t_{z+1}) - W(v,t_z)}{\Delta t} \\
&\qquad \times \int_{t_z}^{t_{z+1}} \exp\left[-\frac{\gamma}{1-\gamma}(t_{n+1} - \kappa)\right] d\kappa + \sigma_{\Delta t}^{n+1}
\end{aligned}
$$

$$= \frac{1}{\gamma\Delta t}\left[1-\exp\left(-\frac{\gamma}{1-\gamma}\Delta t\right)\right] \times \sum_{z=0}^{n}\left[W(v,t_{n-z+1})-W(v,t_{n-z})\right] \times \exp\left(-\frac{\gamma}{1-\gamma}z\Delta t\right)+\sigma_{\Delta t}^{n+1}.$$

Hence,

$$\frac{\partial^\gamma}{\partial t^\gamma}W(v,t_{n+1}) = \frac{\mu}{\gamma\Delta t}\sum_{z=0}^{n} l_z\left[W(v,t_{n-z+1})-W(v,t_{n-z})\right] + \sigma_{\Delta t}^{n+1}, \quad (14)$$

where $\mu = 1-\exp(-\frac{\gamma}{1-\gamma}\Delta t)$ and $l_z = \exp(-\frac{\gamma}{1-\gamma}z\Delta t)$. Moreover, the truncation error $\sigma_{\Delta t}^{n+1}$ is given by[47]

$$|\sigma_{\Delta t}^{n+1}| \le \vartheta(\Delta t)^2, \quad (15)$$

where ϑ is a constant. From the properties of the $\exp(v)$ function, it is straightforward to confirm that

- $l_z > 0$ and $l_0 = 1$, $z = 1:1:n$,
- $l_0 > l_1 > l_2 > \cdots > l_z, l_z \to 0$ as $z \to \infty$,
- $\sum_{z=0}^{n}(l_z - l_{z+1}) + l_{n+1} = (1-l_1) + \sum_{z=1}^{n-1}(l_z - l_{z+1}) + l_n = 1$.

Using (14) and θ-weighted scheme, Eq. (12) can be expressed as

$$\frac{\mu}{\gamma\Delta t}\sum_{z=0}^{n} l_z\left[W(v,t_{n-z+1})-W(v,t_{n-z})\right] = \theta W_{vv}(v,t_{n+1}) + (1-\theta)W_{vv}(v,t_n) + q(v,t_{n+1}). \quad (16)$$

Discretizing (16) for $\theta = 1$, we get

$$W_r^{n+1} - \beta(W_{vv})_r^{n+1} = W_r^n - \sum_{z=1}^{n} l_z[W_r^{n-z+1} - W_r^{n-z}] + \beta\, q_r^{n+1}, \quad r = 0,1,\ldots,N, \quad (17)$$

where $\beta = \frac{\gamma\Delta t}{\mu}$, $W_r^n = W(v_r,t_n)$ and $q_r^{n+1} = q(v_r,t_{n+1})$.

Using (11) in (17), we acquire

$$\begin{aligned}(p_1-\beta p_4)\alpha_{r-1}^{n+1} + (p_2-\beta p_5)\alpha_r^{n+1} + (p_1-\beta p_4)\alpha_{r+1}^{n+1} &= (p_1\alpha_{r-1}^n + p_2\alpha_r^n + p_1\alpha_{r+1}^n) - \sum_{z=1}^{n} l_z\big[p_1(\alpha_{r-1}^{n-z+1} - \alpha_{r-1}^{n-z}) \\ &\quad + p_2(\alpha_r^{n-z+1} - \alpha_r^{n-z}) + p_1(\alpha_{r+1}^{n-z+1} - \alpha_{r+1}^{n-z})\big] + \beta q_r^{n+1}, \\ &\quad r = 0,1,\ldots,N, \end{aligned} \quad (18)$$

where $\alpha_r^n = \alpha_r(t^n)$, $p_1 = \frac{1}{6}$, $p_2 = \frac{4}{6}$, $p_3 = \frac{1}{2h}$, $p_4 = \frac{1}{h^2}$ and $p_5 = \frac{-2}{h^2}$.

The system (18) consists of $N+1$ linear equations in $N+3$ unknowns. To acquire two additional equations for the unique solution, end conditions (3) are utilized. Consequently, a matrix system of dimension $(N+3)\times(N+3)$ is obtained

$$A\alpha^{n+1} = B\left(\sum_{z=0}^{n-1}(l_z - l_{z+1})\alpha^{n-z} + l_n\alpha^0\right) + Q, \quad (19)$$

where

$$A = \begin{pmatrix} p_1 & p_2 & p_1 & & & & \\ p_1-\beta p_4 & p_2-\beta p_5 & p_1-\beta p_4 & & & & \\ & p_1-\beta p_4 & p_2-\beta p_5 & p_1-\beta p_4 & & & \\ & & \ddots & \ddots & \ddots & & \\ & & & p_1-\beta p_4 & p_2-\beta p_5 & p_1-\beta p_4 & \\ & & & & p_1-\beta p_4 & p_2-\beta p_5 & p_1-\beta p_4 \\ & & & & p_1 & p_2 & p_1 \end{pmatrix},$$

$$B=\begin{pmatrix} 0 & 0 & 0 & & & & \\ p_1 & p_2 & p_1 & & & & \\ & p_1 & p_2 & p_1 & & & \\ & & \ddots & \ddots & \ddots & & \\ & & & p_1 & p_2 & p_1 & \\ & & & & p_1 & p_2 & p_1 \\ & & & & 0 & 0 & 0 \end{pmatrix},$$

$$\alpha^n=\begin{pmatrix} \alpha_{-1}^n \\ \alpha_0^n \\ \alpha_1^n \\ \vdots \\ \alpha_{N-1}^n \\ \alpha_N^n \\ \alpha_{N+1}^n \end{pmatrix}$$

and

$$Q=\begin{pmatrix} \phi_1^{n+1} \\ \beta q_0^{n+1} \\ \beta q_1^{n+1} \\ \vdots \\ \beta q_{N-1}^{n+1} \\ \beta q_N^{n+1} \\ \phi_2^{n+1} \end{pmatrix}.$$

Before using (19), the initial vector $\alpha^0=[\alpha_{-1}^0, \alpha_0^0,\ldots,\alpha_{N+1}^0]^T$ is acquired by utilizing the initial conditions as

$$\begin{cases} (W_v)_r^0=\psi'(v_r), & r=0, \\ (W)_r^0=\psi(v_r), & r=0,1,\ldots,N, \\ (W_v)_r^0=\psi'(v_r), & r=N. \end{cases} \tag{20}$$

The above system of equations is represented in matrix form as

$$C\alpha^0=D, \tag{21}$$

where,

$$C=\begin{pmatrix} -p_3 & 0 & p_3 & & & & \\ p_1 & p_2 & p_1 & & & & \\ & p_1 & p_2 & p_1 & & & \\ & & \ddots & \ddots & \ddots & & \\ & & & p_1 & p_2 & p_1 & \\ & & & & p_1 & p_2 & p_1 \\ & & & & -p_3 & 0 & p_3 \end{pmatrix}$$

and

$$D=\begin{pmatrix} \psi'(v_0) \\ \psi(v_0) \\ \psi(v_1) \\ \vdots \\ \psi(v_{N-1}) \\ \psi(v_N) \\ \psi'(v_N) \end{pmatrix}.$$

Equation (21) is easily solvable for α^0 using a suitable numerical algorithm. Mathematica 12 is used to carry out all numerical computations.

4. THE STABILITY ANALYSIS

A numerical scheme is accepted to be stable when the error does not increase during the computational procedure.[48] Here, stability of the scheme is analysed using the Fourier method.[46] Assume that ρ_r^n and $\tilde{\rho}_r^n$ represent the growth factor and its estimation, respectively. The error ζ_r^n can be represented as

$$\zeta_r^n=\rho_r^n-\tilde{\rho}_r^n, \quad r=1(1)N-1, \quad n=0(1)M.$$

To keep the simplicity, we describe the stability of the proposed approach for the linear force-free form of (18) as

$$\begin{aligned}(p_1-\beta p_4)\zeta_{r-1}^{n+1}+(p_2-\beta p_5)\zeta_r^{n+1}+(p_1-\beta p_4)\zeta_{r+1}^{n+1} &= (p_1\zeta_{r-1}^n+p_2\zeta_r^n+p_1\zeta_{r+1}^n) \\ &\quad -\sum_{z=1}^{n} l_z\big[p_1(\zeta_{r-1}^{n-z+1}-\zeta_{r-1}^{n-z})+p_2(\zeta_r^{n-z+1} \\ &\quad -\zeta_r^{n-z})+p_1(\zeta_{r+1}^{n-z+1}-\zeta_{r+1}^{n-z})\big].\end{aligned} \tag{22}$$

From initial and end conditions, we can write

$$\zeta_r^0=\psi(v_r), \quad r=1,2,\ldots,N \tag{23}$$

and

$$\zeta_0^n=\phi_1(t_n), \quad \zeta_N^n=\phi_2(t_n), \quad n=0,1,\ldots,M. \tag{24}$$

We introduce grid function

$$\zeta^n=\begin{cases} \zeta_r^n, & v_r-\dfrac{h}{2}<v\le v_r \\ & +\dfrac{h}{2}, \quad r=1,2,\ldots,N-1, \\ 0, & a\le v\le a+\dfrac{h}{2} \text{ or } b-\dfrac{h}{2}\le v\le b. \end{cases} \tag{25}$$

The Fourier expansion for $\zeta^n(v)$ can be expressed as

$$\zeta^n(v) = \sum_{m=-\infty}^{\infty} \delta^n(m) e^{\frac{2\pi i m v}{b-a}}, \tag{26}$$

where

$$\delta^n(m) = \frac{1}{b-a}\int_a^b \zeta^n(v) e^{\frac{-2\pi i m v}{b-a}} dv, \quad n = 0, 1, 2, \ldots, M \tag{27}$$

and

$$\zeta^n = [\zeta_1^n, \zeta_2^n, \ldots, \zeta_{N-1}^n]^T.$$

Applying $\|.\|_2$ norm, we achieve

$$\begin{aligned}\|\zeta^n\|_2 &= \sqrt{h\sum_{r=1}^{N-1} |\zeta_r^n|^2} \\ &= \left(\int_a^{a+\frac{h}{2}} |\zeta^n|^2 dv + \sum_{r=1}^{N-1}\int_{v_r-\frac{h}{2}}^{v_r+\frac{h}{2}} |\zeta^n|^2 dv \right. \\ &\quad \left. + \int_{b-\frac{h}{2}}^{b} |\zeta^n|^2 dv\right)^{\frac{1}{2}} \\ &= \left(\int_a^b |\zeta^n|^2 dv\right)^{\frac{1}{2}}.\end{aligned}$$

Through Parseval's identity (8), we get[45]

$$\int_a^b |\zeta^n|^2 dv = \sum_{m=-\infty}^{\infty} |\delta^n(m)|^2.$$

Hence, we acquire

$$\|\zeta^n\|_2^2 = \sum_{m=-\infty}^{\infty} |\delta^n(m)|^2. \tag{28}$$

Presume that (22)–(24) possess a solution in the Fourier form as

$$\zeta_r^n = \delta^n e^{i\epsilon r h}, \tag{29}$$

where ϵ is a real number and $i = \sqrt{-1}$. Putting (29) in (22), we achieve

$$\begin{aligned}&(p_1 - \beta p_4)\delta^{n+1} e^{-i\epsilon h} + (p_2 - \beta p_5)\delta^{n+1} \\ &\quad + (p_1 - \beta p_4)\delta^{n+1} e^{i\epsilon h} \\ &= (p_1\delta^n e^{-i\epsilon h} + p_2\delta^n + p_1\delta^n e^{i\epsilon h}) \\ &\quad - \sum_{z=1}^{n} l_z\big[p_1(\delta^{n-z+1}e^{-i\epsilon h} - \delta^{n-z}e^{-i\epsilon h}) \\ &\quad + p_2(\delta^{n-z+1} - \delta^{n-z}) \\ &\quad + p_1(\delta^{n-z+1}e^{i\epsilon h} - \delta^{n-z}e^{i\epsilon h})\big]. \end{aligned} \tag{30}$$

Utilizing the relation $e^{i\epsilon h} + e^{-i\epsilon h} = 2\cos(\epsilon h)$, we acquire

$$\delta^{n+1} = \frac{1}{\eta}\left[\delta^n - \sum_{z=1}^{n} l_z(\delta^{n-z+1} - \delta^{n-z})\right], \tag{31}$$

where $\eta = 1 + \frac{12\beta\sin^2(\epsilon h/2)}{h^2(3-2\sin^2(\epsilon h/2))}$. Obviously $\eta \geq 1$.

Lemma 5. *Assume that δ^n is the solution for* (31)*, then $|\delta^n| \leq |\delta^0|$, $n = 0, 1, \ldots, T \times M$.*

Proof. To examine this, mathematical induction is used. For $n = 0$, (31) implies

$$|\delta^1| = \frac{1}{\eta}|\delta^0| \leq |\delta^0|, \quad \eta \geq 1.$$

Assume that $|\delta^n| \leq |\delta^0|$ for $n = 1, 2, \ldots, T\times(M-1)$, then

$$\begin{aligned}|\delta^{n+1}| &\leq \frac{1}{\eta}|\delta^n| - \frac{1}{\eta}\sum_{z=1}^{n} l_z\big(|\delta^{n-z+1}| - |\delta^{n-z}|\big) \\ &\leq \frac{1}{\eta}|\delta^0| - \frac{1}{\eta}\sum_{z=1}^{n} l_z\big(|\delta^0| - |\delta^0|\big) \\ &\leq |\delta^0|.\end{aligned}$$

□

Theorem 6. *The scheme* (18) *is unconditionally stable.*

Proof. Employing the expression (28) and Lemma 5, we achieve

$$\|\zeta^n\|_2 \leq \|\zeta^0\|_2, \quad n = 0, 1, \ldots, M.$$

Thus, the presented scheme is stable unconditionally. □

5. THE CONVERGENCE ANALYSIS

To investigate convergence of the proposed method, we follow the procedure described in Ref. 49. Firstly, some useful theorems and lemmas are brought forward.[50,51]

Theorem 7. *Assuming $w(v,t)$, q belong to $C^4[a,b]$ and $C^2[a,b]$, respectively, and $\Psi = \{a = v_0, v_1, \ldots, v_N = b\}$ is the partition of $[a,b]$ s.t. $v_r = a + rh, r = 0, 1, \ldots, N$. If $\tilde{W}(v,t)$ is the CBS approximation*

to (1) *at points* $v_r \in \Psi$, *then there exists* Ω_r *not depending on* h, *we have*

$$\|D^r\big(w(v,t)-\tilde{W}(v,t)\big)\|_\infty \le \Omega_r h^{4-r}, \quad \forall\, t \ge 0, \quad r=0,1,2. \tag{32}$$

Lemma 8. *The CBS set* $\{S_{-1}, S_0, \ldots, S_{N+1}\}$ *presented in* (10) *satisfies the inequality*

$$\sum_{r=-1}^{N+1} |S_r(v)| \le \frac{5}{3}, \quad 0 \le v \le 1. \tag{33}$$

Proof. We can write the following relation using the triangular inequality:

$$\left|\sum_{r=-1}^{N+1} S_r(v)\right| \le \sum_{r=-1}^{N+1} |S_r(v)|.$$

At any knot v_r, we acquire

$$\sum_{r=-1}^{N+1} |S_r(v)| = |S_{r-1}(v_r)| + |S_r(v_r)| + |S_{r+1}(v_r)| = \frac{1}{6}+\frac{4}{6}+\frac{1}{6} = 1 < \frac{5}{3}.$$

Moreover, for $v \in [v_r, v_{r+1}]$, we get

$$|S_r(v)| \le \frac{4}{6}, \quad |S_{r-1}(v)| \le \frac{1}{6},$$

$$|S_{r+1}(v)| \le \frac{4}{6} \quad \text{and} \quad |S_{r+2}(v)| \le \frac{1}{6}.$$

Hence, for any point $v_r \le v \le v_{r+1}$, we attain

$$\sum_{r=-1}^{N+1} |S_r(v)| = |S_{r-1}(v)| + |S_r(v)| + |S_{r+1}(v)| + |S_{r+2}(v)| \le \frac{5}{3}. \qquad \square$$

Theorem 9. *The numerical approximation* $W(v,t)$ *to the exact solution* $w(v,t)$ *for TFDE exists. Furthermore, if* q *is a member of* $C^2[0,1]$, *then*

$$\|w(v,t)-W(v,t)\|_\infty \le \widetilde{\Omega} h^2, \quad \forall\, t \ge 0, \tag{34}$$

where $\widetilde{\Omega} > 0$ *is free of* h *and* h *is appropriately small.*

Proof. We suppose that $\tilde{W}(v,t) = \sum_{r=-1}^{N+1} a_r^n(t)\, S_r(v)$ be the approximated CBS for $W(v,t)$. By implementing the triangular inequality, we obtain

$$\|w(v,t)-W(v,t)\|_\infty \le \|w(v,t)-\tilde{W}(v,t)\|_\infty + \|\tilde{W}(v,t)-W(v,t)\|_\infty.$$

Making use of Theorem 7, we get

$$\|w(v,t)-W(v,t)\|_\infty \le \Omega_0 h^4 + \|\tilde{W}(v,t)-W(v,t)\|_\infty. \tag{35}$$

$Lw(v_r,t) = LW(v_r,t) = q(v_r,t)$, $r = 0(1)N$ are the collocation conditions. Assume that

$$L\tilde{W}(v_r,t) = \tilde{q}(v_r,t), \quad r = 0(1)N.$$

Thus, for any time stage n, the difference $L(\tilde{W}(v_r,t)-W(v_r,t))$ can be stated as

$$\begin{aligned}
&(p_1-\beta p_4)\chi_{r-1}^{n+1} + (p_2-\beta p_5)\chi_r^{n+1} + (p_1-\beta p_4)\chi_{r+1}^{n+1} \\
&= (p_1\chi_{r-1}^n + p_2\chi_r^n + p_1\chi_{r+1}^n) + \frac{\beta}{h^2}\ \xi_r^{n+1} \\
&\quad - \sum_{z=1}^{n} l_z\big[p_1(\chi_{r-1}^{n-z+1} - \chi_{r-1}^{n-z}) + p_2(\chi_r^{n-z+1} - \chi_r^{n-z}) \\
&\quad + p_1(\chi_{r+1}^{n-z+1} - \chi_{r+1}^{n-z})\big].
\end{aligned} \tag{36}$$

The end conditions can be described as

$$p_1\chi_{r-1}^{n+1} + p_2\chi_r^{n+1} + p_1\chi_{r+1}^{n+1} = 0, \quad r = 0, N,$$

where

$$\chi_r^n = \alpha_r^n - a_r^n, \quad r = -1:0:N+1$$

and

$$\xi_r^n = h^2[q_r^n - \tilde{q}_r^n], \quad r = 0:1:N.$$

From inequality (32), we achieve

$$|\xi_r^n| = h^2|q_r^n - \tilde{q}_r^n| \le \Omega h^4.$$

Define $\xi^n = max\{|\xi_r^n|; 0 \le r \le N\}$, $E_r^n = |\chi_r^n|$ and $E^n = max\{|E_r^n|; 0 \le r \le N\}$.

When $n = 0$, Eq. (36) becomes

$$(p_1-\beta p_4)\chi_{r-1}^1 + (p_2-\beta p_5)\chi_r^1 + (p_1-\beta p_4)\chi_{r+1}^1 = (p_1\chi_{r-1}^0 + p_2\chi_r^0 + p_1\chi_{r+1}^0) + \frac{\beta}{h^2}\xi_r^1,$$

where $r = 0:1:N$. Through initial condition, $E^0 = 0$:

$$(p_2-\beta p_5)\chi_r^1 = -(p_1-\beta p_4)(\chi_{r-1}^1 + \chi_{r+1}^1) + \frac{\beta}{h^2}\xi_r^1.$$

Taking norms of χ_r^1, ξ_r^1 and adequately small grid spacing h, we have

$$E_r^1 \le \frac{3\beta}{h^2+12\beta}\Omega h^4, \quad r = 0:1:N.$$

The values of E^1_{-1} and E^1_{N+1} are obtained from the end conditions:

$$E^1_{-1} \leq \frac{15\beta}{h^2+12\beta}\Omega h^4,$$

$$E^1_{N+1} \leq \frac{15\beta}{h^2+12\beta}\Omega h^4,$$

which implies

$$E^1 \leq \Omega_1 h^2, \tag{37}$$

where Ω_1 does not reliant on h.

Now, mathematical induction on n is used. Assume that $E^s_r \leq \Omega_s h^2$ is true for $s = 1, 2, \ldots, n$ and $\Omega = \max\{\Omega_s : s = 0, 1, \ldots, n\}$, then from Eq. (36), we acquire

$$\begin{aligned}(p_1-\beta p_4)\chi^{n+1}_{r-1} &+ (p_2-\beta p_5)\chi^{n+1}_r + (p_1-\beta p_4)\\ &\times \chi^{n+1}_{r+1}\\ &= \big[(l_0-l_1)(p_1\chi^n_{r-1}+p_2\chi^n_r+p_1\chi^n_{r+1})\\ &+ (l_1-l_2)(p_1\chi^{n-1}_{r-1}+p_2\chi^{n-1}_r+p_1\chi^{n-1}_{r+1})\\ &+ \cdots + (l_{n-1}-l_n)(p_1\chi^1_{r-1}+p_2\chi^1_r\\ &+ p_1\chi^1_{r+1}) + l_n(p_1\chi^0_{r-1}+p_2\chi^0_r+p_1\chi^0_{r+1})\big]\\ &+ \frac{\beta}{h^2}\xi^{n+1}_r.\end{aligned}$$

Again, applying the norms on χ^{n+1}_r and ξ^{n+1}_r, we get

$$E^{n+1}_r \leq \frac{3\Omega h^4}{h^2+12\beta}\left(\beta + \sum_{z=0}^{n-1}(l_z - l_{z+1})\right).$$

Similarly, we obtain the values of E^{n+1}_{-1} and E^{n+1}_{N+1} from the end conditions:

$$E^{n+1}_{-1} \leq \frac{15\Omega h^4}{h^2+12\beta}\left(\beta + \sum_{z=0}^{n-1}(l_z - l_{z+1})\right),$$

$$E^{n+1}_{N+1} \leq \frac{15\Omega h^4}{h^2+12\beta}\left(\beta + \sum_{z=0}^{n-1}(l_z - l_{z+1})\right).$$

Hence, for all n, we acquire

$$E^{n+1} \leq \Omega h^2. \tag{38}$$

In particular,

$$\tilde{W}(v,t) - W(v,t) = \sum_{r=-1}^{N+1}\big(a_r(t) - \alpha_r(t)\big)S_r(v).$$

Therefore, from inequality (38) and Lemma 8, we get

$$\|\tilde{W}(v,t) - W(v,t)\|_\infty \leq \frac{5}{3}\Omega h^2. \tag{39}$$

Employing (39), the inequality (35) becomes

$$\|w(v,t) - W(v,t)\|_\infty \leq \Omega_0 h^4 + \frac{5}{3}\Omega h^2 = \widetilde{\Omega} h^2,$$

where $\widetilde{\Omega} = \Omega_0 h^2 + \frac{5}{3}\Omega$. □

Theorem 10. *The TFDE is convergent with initial and end conditions.*

Proof. Assume that $w(v,t)$ and $W(v,t)$ are analytical and numerical solutions for the TFDE, respectively. As a result of relation (15) and the preceding theorem, there exist arbitrary constants $\widetilde{\Omega}$ and ϑ such that

$$\|w(v,t) - W(v,t)\|_\infty \leq \widetilde{\Omega} h^2 + \vartheta(\Delta t)^2.$$

Consequently, in spatial and temporal directions, the presented method is second-order convergent. □

6. NUMERICAL EXAMPLES AND DISCUSSION

In this section, numerical outcomes of some experiments using presented method are reported. The computational efficiency of the technique is checked through the error norms $e_2(h,\Delta t)$ and $e_\infty(h,\Delta t)$ as

$$\begin{aligned}e_2(h,\Delta t) &= \|w(v_r,t) - W(v_r,t)\|_2\\ &= \sqrt{h\sum_{r=0}^{N}|w(v_r,t) - W(v_r,t)|^2}\end{aligned}$$

and

$$\begin{aligned}e_\infty(h,\Delta t) &= \|w(v_r,t) - W(v_r,t)\|_\infty\\ &= \max_{0\leq r\leq N}|w(v_r,t) - W(v_r,t)|.\end{aligned}$$

Moreover, the convergence order in spatial and temporal directions is computed as[47]

$$\log_2\left|\frac{e_\infty(h,\Delta t)}{e_\infty(\frac{h}{2},\Delta t)}\right| \text{ and } \log_2\left|\frac{e_\infty(h,\Delta t)}{e_\infty(h,\frac{\Delta t}{2})}\right|.$$

Example 11. Consider the TFDE[47]

$$\frac{\partial^\gamma w(v,t)}{\partial t^\gamma} = \frac{\partial^2 w(v,t)}{\partial v^2} + q(v,t), \quad v\in[0,1], \quad t\in[0,1],$$

with initial and end conditions

$$w(v,0) = e^{\gamma v}$$

and

$$w(0,t) = e^t, \quad w(1,t) = e^{\gamma+t},$$

where $q(v,t) = -e^{\gamma v+t}\big(e^{-\frac{1}{1-\gamma}t} + \gamma^2 - 1\big)$.

Table 1 Absolute Error When $t = 1$, $\gamma = 0.1$, $\Delta t = 0.01$ and $N = 10$ of Example 11.

v	Exact Solution	Approximate Solution	Absolute Error
0.1	2.7456010150169163	2.7456010773020605	6.22851×10^{-8}
0.2	2.7731947639642978	2.7731948744068227	1.10443×10^{-7}
0.3	2.8010658346990790	2.8010659795360200	1.44837×10^{-7}
0.4	2.8292170143515600	2.8292171800365207	1.65685×10^{-7}
0.5	2.8576511180631640	2.8576512911203724	1.73057×10^{-7}
0.6	2.8863709892679585	2.8863711561470584	1.66879×10^{-7}
0.7	2.9153794999769970	2.9153796469070320	1.46930×10^{-7}
0.8	2.9446795510655240	2.9446796639065513	1.12841×10^{-7}
0.9	2.9742740725630656	2.9742741366538230	6.40908×10^{-8}

Table 2 Absolute Error When $t = 1$, $N = 20$, $\gamma = 0.3$ and $\Delta t = 0.01$ of Example 11.

v	Exact Solution	Approximate Solution	Absolute Error
0.1	2.8010658346990790	2.8010659598562370	1.25157×10^{-7}
0.2	2.8863709892679585	2.8863712124252214	2.23157×10^{-7}
0.3	2.9742740725630656	2.9742743670020357	2.94439×10^{-7}
0.4	3.0648542032930024	3.0648545423483250	3.39055×10^{-7}
0.5	3.1581929096897670	3.1581932663632020	3.56673×10^{-7}
0.6	3.2543742028896707	3.2543745494587630	3.46569×10^{-7}
0.7	3.3534846525490236	3.3534849601651650	3.07616×10^{-7}
0.8	3.4556134647626755	3.4556137030331793	2.38271×10^{-7}
0.9	3.5608525623555205	3.5608526989041350	1.36549×10^{-7}

Table 3 Error Norms for Different γ Choices with $\Delta t = 0.01$ and $N = 32$ for Example 11.

	$e_\infty(h, \Delta t)$		$e_2(h, \Delta t)$	
t	$\gamma = 0.3$	$\gamma = 0.5$	$\gamma = 0.3$	$\gamma = 0.5$
0.2	3.50778×10^{-8}	3.98217×10^{-7}	2.57441×10^{-8}	2.91972×10^{-7}
0.4	1.69987×10^{-7}	1.20488×10^{-7}	1.24707×10^{-7}	8.79828×10^{-8}
0.6	3.25632×10^{-7}	1.62955×10^{-7}	2.38850×10^{-7}	1.19994×10^{-7}
0.8	5.07259×10^{-7}	4.61873×10^{-7}	3.72020×10^{-7}	3.39143×10^{-7}
1.0	7.21229×10^{-7}	7.86892×10^{-7}	5.28880×10^{-7}	5.77290×10^{-7}

The exact solution is $w(v,t) = e^{\gamma v + t}$. Absolute errors are reported in Tables 1 and 2 for Example 11 when $t = 1$, $\Delta t = 0.01$, $\gamma = 0.1, 0.3$ and $N = 10, 20$, respectively. At different time intervals, error norms are listed in Table 3. Table 4 shows the comparison of maximum error with the results given in Ref. 47 at $t = 1$ of Example 11 for different γ choices. Table 5 compares convergence order and error by setting $\gamma = 0.5$ at $t = 1$. The plots of exact and computational results at various time stages for $N = 16, 100$, $\gamma = 0.5$ and $\Delta t = 0.01$ are depicted in Fig. 1. Figure 2 shows the accuracy of the current scheme through 3D graphs of analytical and numerical solutions. At $t = 1$, 2D and 3D error profiles are displayed in Fig. 3. Figure 4 illustrates the numerical and exact solutions when $N = 20, 100$ and $\Delta t = 0.01$ by setting different choices of γ at $t = 1$. In comparison to the scheme presented in Ref. 47, the proposed scheme is found to be more efficient and accurate. The numerical solutions using CBS approximations when $\gamma = 0.5, 0.75$, $t = 0.5, 1$, $\Delta t = 0.01$, $0 \leq v \leq 1$ and $h = 0.02, 0.05$ are

Table 4 Maximum Error's Comparison When $t = 1$ for Example 11.

		FDM[47]			**Proposed Method**		
h	Δt	$\gamma = 0.25$	$\gamma = 0.75$	$\gamma = 0.95$	$\gamma = 0.25$	$\gamma = 0.75$	$\gamma = 0.95$
0.05	0.05	1.78606×10^{-5}	3.00280×10^{-4}	2.05777×10^{-3}	1.73054×10^{-5}	2.41731×10^{-4}	1.88707×10^{-3}
	0.02	3.54460×10^{-6}	3.30745×10^{-5}	4.06247×10^{-4}	2.53244×10^{-6}	1.37860×10^{-5}	2.34313×10^{-4}
	0.01	9.84836×10^{-7}	4.05129×10^{-5}	1.66279×10^{-4}	4.21817×10^{-7}	1.88081×10^{-5}	5.83444×10^{-6}
0.02	0.05	1.76317×10^{-5}	2.76236×10^{-4}	1.98642×10^{-3}	1.75429×10^{-5}	2.66772×10^{-4}	1.95910×10^{-3}
	0.02	2.85917×10^{-6}	4.82200×10^{-5}	3.34114×10^{-4}	2.76922×10^{-6}	3.87260×10^{-5}	3.06600×10^{-4}
	0.01	7.48608×10^{-7}	1.56190×10^{-5}	9.40322×10^{-5}	6.58504×10^{-7}	6.11960×10^{-6}	6.64896×10^{-5}
0.01	0.05	1.76032×10^{-5}	2.72688×10^{-4}	1.97617×10^{-3}	1.75809×10^{-5}	2.70322×10^{-4}	1.96935×10^{-3}
	0.02	2.82620×10^{-6}	4.46604×10^{-5}	3.23797×10^{-4}	2.80371×10^{-6}	4.22867×10^{-5}	3.16918×10^{-4}
	0.01	7.15013×10^{-7}	1.20570×10^{-5}	8.37043×10^{-5}	6.92481×10^{-7}	9.68207×10^{-6}	7.68187×10^{-5}

given by

$$W(v,0.5) = \begin{cases} 1.64872 + v(0.824363 + (0.206086 + 0.0345207v)v) & \text{if } v \in [0.00, 0.02) \\ 1.64872 + v(0.824364 + (0.206065 + 0.0348676v)v) & \text{if } v \in [0.02, 0.04) \\ 1.64872 + v(0.824365 + (0.206023 + 0.035218v)v) & \text{if } v \in [0.04, 0.06) \\ 1.64872 + v(0.824369 + (0.205959 + 0.0355719v)v) & \text{if } v \in [0.06, 0.08) \\ 1.64872 + v(0.824376 + (0.205873 + 0.0359294v)v) & \text{if } v \in [0.08, 0.10) \\ 1.64872 + v(0.824387 + (0.205765 + 0.0362904v)v) & \text{if } v \in [0.10, 0.12) \\ 1.64872 + v(0.824403 + (0.205634 + 0.0366551v)v) & \text{if } v \in [0.12, 0.14) \\ 1.64872 + v(0.824424 + (0.205479 + 0.0370235v)v) & \text{if } v \in [0.14, 0.16) \\ \quad \vdots & \\ 1.64847 + v(0.826491 + (0.199424 + 0.0434469v)v) & \text{if } v \in [0.46, 0.48) \\ 1.64842 + v(0.826793 + (0.198795 + 0.0438835v)v) & \text{if } v \in [0.48, 0.50) \\ 1.64837 + v(0.827123 + (0.198133 + 0.0443245v)v) & \text{if } v \in [0.50, 0.52) \\ 1.6483 + v(0.827485 + (0.197438 + 0.0447699v)v) & \text{if } v \in [0.52, 0.54) \\ \quad \vdots & \\ 1.64557 + v(0.838914 + (0.181261 + 0.0525374v)v) & \text{if } v \in [0.84, 0.86) \\ 1.64523 + v(0.840085 + (0.179899 + 0.0530654v)v) & \text{if } v \in [0.86, 0.88) \\ 1.64487 + v(0.841324 + (0.178491 + 0.0535987v)v) & \text{if } v \in [0.88, 0.90) \\ 1.64447 + v(0.842633 + (0.177036 + 0.0541373v)v) & \text{if } v \in [0.90, 0.92) \\ 1.64405 + v(0.844015 + (0.175535 + 0.0546814v)v) & \text{if } v \in [0.92, 0.94) \\ 1.64359 + v(0.845471 + (0.173985 + 0.0552309v)v) & \text{if } v \in [0.94, 0.96) \\ 1.6431 + v(0.847006 + (0.172387 + 0.0557859v)v) & \text{if } v \in [0.96, 0.98) \\ 1.64258 + v(0.848621 + (0.170738 + 0.0563466v)v) & \text{if } v \in [0.98, 1.00) \end{cases} \tag{40}$$

Table 5 Error Norm's Comparison for Example 11 When $t = 1$ and $\gamma = 0.5$.

		FDM[47]		Proposed Method		
h	Δt	$e_\infty(h, \Delta t)$	Order	$e_\infty(h, \Delta t)$	$e_2(h, \Delta t)$	Order
0.05	0.02	1.61978×10^{-5}	⋯	6.01029×10^{-6}	4.41463×10^{-6}	⋯
	0.01	7.87199×10^{-6}	1.04100	2.32171×10^{-6}	1.70262×10^{-6}	1.37225
0.02	0.02	1.19452×10^{-5}	⋯	1.03118×10^{-5}	7.55533×10^{-6}	⋯
	0.01	3.59933×10^{-6}	1.73063	1.96501×10^{-6}	1.43997×10^{-6}	2.39169
0.01	0.02	1.13327×10^{-5}	⋯	1.09244×10^{-5}	8.00390×10^{-6}	⋯
	0.01	2.98650×10^{-6}	1.92396	2.57792×10^{-6}	1.88881×10^{-6}	2.08327

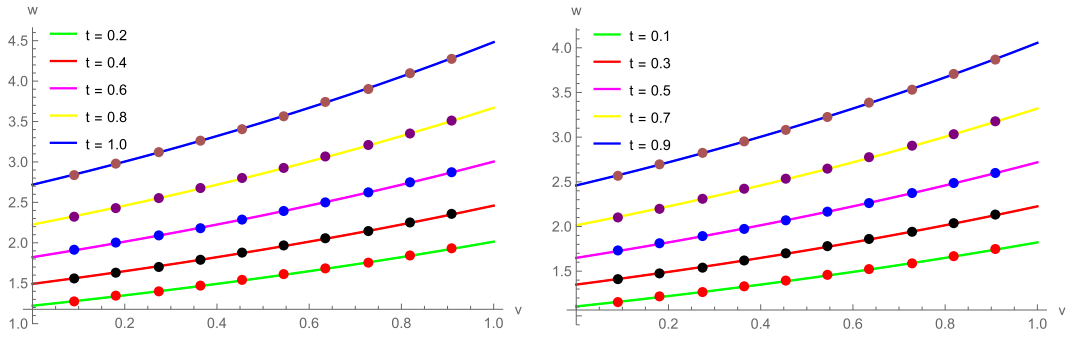

(a) $N = 16$ **(b)** $N = 100$

Fig. 1 Exact and approximate solutions at various time levels with $\Delta t = 0.01$ and $\gamma = 0.5$ for Example 11.

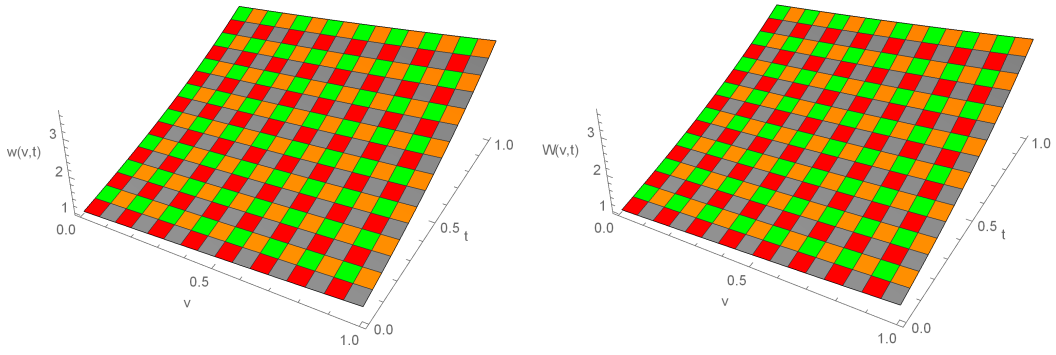

(a) Exact Solution **(b)** Approximate Solution

Fig. 2 3D exact and approximate solutions with $N = 100$, $\gamma = 0.3$, $t = 1$, $v \in [0, 1]$ and $\Delta t = 0.01$ for Example 11.

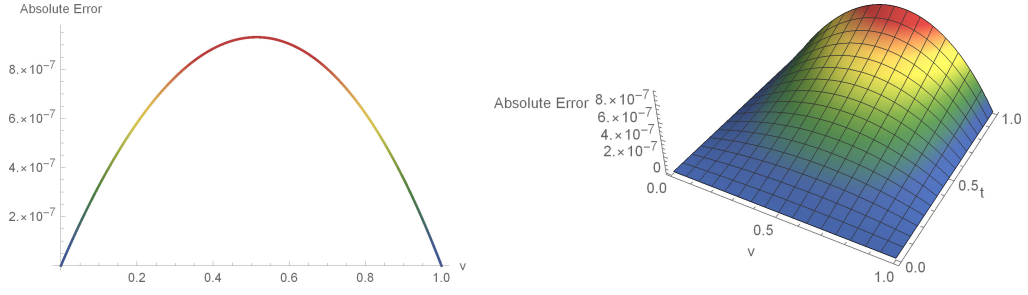

(a) 2D Error Function **(b)** 3D Error Function

Fig. 3 2D and 3D error profiles with $N = 100$, $\gamma = 0.3$, $v \in [0, 1]$, $t = 1$ and $\Delta t = 0.01$ for Example 11.

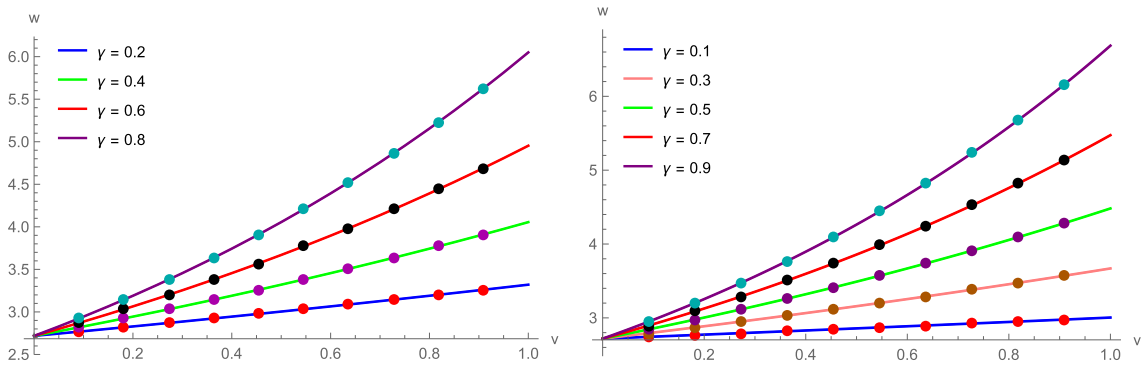

(a) $N = 20$ **(b)** $N = 100$

Fig. 4 Exact and approximate solutions at various γ values for Example 11 with $\Delta t = 0.01$ and $t = 1$.

and

$$W(v,1) = \begin{cases} 2.71828 + v(2.03864 + (0.76448 + 0.19474v)v) & \text{if } v \in [0.00, 0.05) \\ 2.71828 + v(2.0387 + (0.763367 + 0.202182v)v) & \text{if } v \in [0.05, 0.10) \\ 2.71827 + v(2.03893 + (0.761049 + 0.209909v)v) & \text{if } v \in [0.10, 0.15) \\ 2.71825 + v(2.03947 + (0.757439 + 0.217931v)v) & \text{if } v \in [0.15, 0.20) \\ 2.71818 + v(2.04047 + (0.752442 + 0.22626v)v) & \text{if } v \in [0.20, 0.25) \\ 2.71804 + v(2.04209 + (0.745956 + 0.234907v)v) & \text{if } v \in [0.25, 0.30) \\ 2.7178 + v(2.04452 + (0.737876 + 0.243885v)v) & \text{if } v \in [0.30, 0.35) \\ 2.7174 + v(2.04794 + (0.72809 + 0.253205v)v) & \text{if } v \in [0.35, 0.40) \\ 2.71678 + v(2.05259 + (0.716478 + 0.262882v)v) & \text{if } v \in [0.40, 0.45) \\ 2.71587 + v(2.05869 + (0.702915 + 0.272928v)v) & \text{if } v \in [0.45, 0.50) \\ 2.71456 + v(2.06651 + (0.687269 + 0.283359v)v) & \text{if } v \in [0.50, 0.55) \\ 2.71276 + v(2.07634 + (0.669401 + 0.294188v)v) & \text{if } v \in [0.55, 0.60) \\ 2.71033 + v(2.08848 + (0.649164 + 0.305431v)v) & \text{if } v \in [0.60, 0.65) \\ 2.70713 + v(2.10328 + (0.626403 + 0.317103v)v) & \text{if } v \in [0.65, 0.70) \\ 2.70297 + v(2.12109 + (0.600954 + 0.329221v)v) & \text{if } v \in [0.70, 0.75) \\ 2.69766 + v(2.14232 + (0.572646 + 0.341803v)v) & \text{if } v \in [0.75, 0.80) \\ 2.69098 + v(2.1674 + (0.541297 + 0.354865v)v) & \text{if } v \in [0.80, 0.85) \\ 2.68265 + v(2.1968 + (0.506715 + 0.368427v)v) & \text{if } v \in [0.85, 0.90) \\ 2.67238 + v(2.23101 + (0.4687 + 0.382506v)v) & \text{if } v \in [0.90, 0.95) \\ 2.65985 + v(2.27059 + (0.427039 + 0.397124v)v) & \text{if } v \in [0.95, 1.00). \end{cases} \tag{41}$$

Example 12. Consider the TFDE[47]

$$\frac{\partial^\gamma w(v,t)}{\partial t^\gamma} = \frac{\partial^2 w(v,t)}{\partial v^2} + q(v,t), \quad v \in [0,1], \quad t \in [0,5],$$

with initial and end conditions

$$w(v,0) = \cos \gamma v$$

and

$$w(0,t) = 1 + \sin \frac{\gamma}{1-\gamma} t,$$

$$w(1,t) = \cos \gamma + \sin \frac{\gamma}{1-\gamma} t,$$

where $q(v,t) = \gamma^2 \cos \gamma v + \frac{1}{2-2\gamma}\big(\cos(\frac{\gamma}{1-\gamma}t) + \sin(\frac{\gamma}{1-\gamma}t) - \exp(-\frac{\gamma}{1-\gamma}t)\big)$.

The exact solution is $w(v,t) = \cos \gamma v + \sin \frac{\gamma}{1-\gamma} t$. The numerical results and absolute errors for Example 12 at various spatial grid points with $N = 100$, $\gamma = 0.3, 0.5$ and $\Delta t = 0.01$ at $t = 1, 4$ are shown in Tables 6 and 7. Error norms for various γ values are displayed in Table 8 at different time stages. Table 9 compares the maximum relative error at various time stages with $\gamma = 0.5$. The maximum absolute error $e_\infty(h, \Delta t)$ for $\gamma = 0.5$, $\Delta t = 0.01$ and $h = 0.02, 0.01$ is reported in Tables 10 and 11. Tables 12 and 13 compare error and convergence order with those obtained in Ref. 47 along temporal and spatial grids, respectively. The close agreement between exact solutions and numerical results of the proposed scheme at various time levels can be seen in Fig. 5. Comparison of computational and exact solutions is displayed in Fig. 6 for $N = 32$, $\Delta t = 0.01$, $\gamma = 0.5$, $t = 5$ and $v \in [0, 1]$. At $t = 5$, 2D and 3D error profiles are demonstrated in Fig. 7. Figure 8 exhibits the behavior of exact values and computational results for various γ choices. The approximate solutions using CBS approximations with $\gamma = 0.5, 0.3$, $0 \le v \le 1$, $t = 1, 5$, $h = 0.02, 0.05$ and $\Delta t = 0.01$ are given by

$$W(v,1) = \begin{cases} 1.84147 + v(-3.45765 \times 10^{-6} + (-0.124997 + 0.000103466v)v) & \text{if } v \in [0.00, 0.02) \\ 1.84147 + v(-3.20762 \times 10^{-6} + (-0.12501 + 0.000311818v)v) & \text{if } v \in [0.02, 0.04) \\ 1.84147 + v(-2.20769 \times 10^{-6} + (-0.125035 + 0.000520139v)v) & \text{if } v \in [0.04, 0.06) \\ 1.84147 + v(4.16136 \times 10^{-8} + (-0.125072 + 0.000728407v)v) & \text{if } v \in [0.06, 0.08) \\ 1.84147 + v(4.03896 \times 10^{-6} + (-0.125122 + 0.000936602v)v) & \text{if } v \in [0.08, 0.10) \\ 1.84147 + v(0.000010282 + (-0.125185 + 0.0011447v)v) & \text{if } v \in [0.10, 0.12) \\ 1.84147 + v(0.000019267 + (-0.125259 + 0.00135269v)v) & \text{if } v \in [0.12, 0.14) \\ 1.84147 + v(0.0000314886 + (-0.125347 + 0.00156054v)v) & \text{if } v \in [0.14, 0.16) \\ \quad \vdots & \\ 1.84135 + v(0.00105985 + (-0.1284 + 0.00485084v)v) & \text{if } v \in [0.46, 0.48) \\ 1.84132 + v(0.00119974 + (-0.128692 + 0.00505322v)v) & \text{if } v \in [0.48, 0.50) \\ 1.8413 + v(0.00135115 + (-0.128994 + 0.00525511v)v) & \text{if } v \in [0.50, 0.52) \\ 1.84127 + v(0.00151449 + (-0.129309 + 0.00545646v)v) & \text{if } v \in [0.52, 0.54) \\ \quad \vdots & \\ 1.84019 + v(0.00605082 + (-0.135782 + 0.00859047v)v) & \text{if } v \in [0.84, 0.86) \\ 1.84007 + v(0.00647105 + (-0.13627 + 0.00877986v)v) & \text{if } v \in [0.86, 0.88) \\ 1.83994 + v(0.00690901 + (-0.136768 + 0.00896838v)v) & \text{if } v \in [0.88, 0.90) \\ 1.83981 + v(0.00736493 + (-0.137274 + 0.009156v)v) & \text{if } v \in [0.90, 0.92) \\ 1.83966 + v(0.00783901 + (-0.13779 + 0.00934271v)v) & \text{if } v \in [0.92, 0.94) \\ 1.83951 + v(0.00833146 + (-0.138314 + 0.00952848v)v) & \text{if } v \in [0.94, 0.96) \\ 1.83934 + v(0.00884245 + (-0.138846 + 0.0097133v)v) & \text{if } v \in [0.96, 0.98) \\ 1.83917 + v(0.00937215 + (-0.139386 + 0.00989715v)v) & \text{if } v \in [0.98, 1.00) \end{cases} \quad (42)$$

Table 6 Absolute Error at Different Spatial Grid Points When $t = 1$, $\Delta t = 0.01$, $\gamma = 0.3$ and $N = 100$ for Example 12.

v	Exact Solution	Approximate Solution	Absolute Error
0.1	1.4151218887420396	1.4151218789931579	9.74888×10^{-9}
0.2	1.4137723949282561	1.4137723777162572	1.72120×10^{-8}
0.3	1.4115245880050462	1.4115245655286313	2.24764×10^{-8}
0.4	1.4083804908469182	1.4083804652424539	2.56045×10^{-8}
0.5	1.4043429329290942	1.4043429062946715	2.66344×10^{-8}
0.6	1.3994155477811734	1.3994155222002440	2.55809×10^{-8}
0.7	1.3936027697172002	1.3936027472820223	2.24352×10^{-8}
0.8	1.3869098298450815	1.3869098126803014	1.71648×10^{-8}
0.9	1.3793427513589425	1.3793427416455640	9.71338×10^{-9}

and

$$W(v,5) = \begin{cases} 1.84079 + v(-1.60668 \times 10^{-6} + (-0.0449992 + 0.0000336533v)v) & \text{if } v \in [0.00, 0.05) \\ 1.84079 + v(-1.10042 \times 10^{-6} + (-0.0450093 + 0.000101155v)v) & \text{if } v \in [0.05, 0.10) \\ 1.84079 + v(9.23936 \times 10^{-7} + (-0.0450295 + 0.000168633v)v) & \text{if } v \in [0.10, 0.15) \\ 1.84079 + v(5.47617 \times 10^{-6} + (-0.0450599 + 0.000236073v)v) & \text{if } v \in [0.15, 0.20) \\ 1.84079 + v(0.0000135627 + (-0.0451003 + 0.000303461v)v) & \text{if } v \in [0.20, 0.25) \\ 1.84079 + v(0.000026185 + (-0.0451508 + 0.00037078v)v) & \text{if } v \in [0.25, 0.30) \\ 1.84078 + v(0.0000443386 + (-0.0452113 + 0.000438016v)v) & \text{if } v \in [0.30, 0.35) \\ 1.84078 + v(0.0000690115 + (-0.0452818 + 0.000505153v)v) & \text{if } v \in [0.35, 0.40) \\ 1.84078 + v(0.000101183 + (-0.0453623 + 0.000572176v)v) & \text{if } v \in [0.40, 0.45) \\ 1.84077 + v(0.000141821 + (-0.0454526 + 0.000639071v)v) & \text{if } v \in [0.45, 0.50) \\ 1.84076 + v(0.000191885 + (-0.0455527 + 0.000705822v)v) & \text{if } v \in [0.50, 0.55) \\ 1.84075 + v(0.000252317 + (-0.0456626 + 0.000772414v)v) & \text{if } v \in [0.55, 0.60) \\ 1.84074 + v(0.000324049 + (-0.0457821 + 0.000838832v)v) & \text{if } v \in [0.60, 0.65) \\ 1.84074 + v(0.000324049 + (-0.0457821 + 0.000838832v)v) & \text{if } v \in [0.65, 0.70) \\ 1.8407 + v(0.000505053 + (-0.0460499 + 0.000971088v)v) & \text{if } v \in [0.70, 0.75) \\ 1.84067 + v(0.000616103 + (-0.046198 + 0.0010369v)v) & \text{if } v \in [0.75, 0.80) \\ 1.84063 + v(0.000742005 + (-0.0463554 + 0.00110247v)v) & \text{if } v \in [0.80, 0.85) \\ 1.84059 + v(0.000883599 + (-0.0465219 + 0.0011678v)v) & \text{if } v \in [0.85, 0.90) \\ 1.84055 + v(0.0010417 + (-0.0466976 + 0.00123286v)v) & \text{if } v \in [0.90, 0.95) \\ 1.84049 + v(0.00121711 + (-0.0468823 + 0.00129764v)v) & \text{if } v \in [0.95, 1.00). \end{cases} \tag{43}$$

Example 13. Consider the TFDE[47]

$$\frac{\partial^\gamma w(v,t)}{\partial t^\gamma} = \frac{\partial^2 w(v,t)}{\partial v^2} + q(v,t), \quad v \in [0,1], \quad t \in [0,1],$$

Table 7 Absolute Error at Different Spatial Grid Points When $t = 4$, $\Delta t = 0.01$, $\gamma = 0.5$ and $N = 100$ for Example 12.

v	Exact Solution	Approximate Solution	Absolute Error
0.1	0.2419477650870381	0.2419477255887654	3.94983×10^{-8}
0.2	0.2382016699700976	0.2382015944086032	7.55615×10^{-8}
0.3	0.2319685826281140	0.2319684785434553	1.04085×10^{-7}
0.4	0.2232640825333134	0.2232639603306453	1.22203×10^{-7}
0.5	0.2121099264027165	0.2121097981611280	1.28242×10^{-7}
0.6	0.1985339938176778	0.1985338721281287	1.21690×10^{-7}
0.7	0.1825702175394507	0.1825701143524707	1.03187×10^{-7}
0.8	0.1642584986949569	0.1642584241588478	7.45361×10^{-8}
0.9	0.1436446070447487	0.1436445683149489	3.87298×10^{-8}

Table 8 Error Norms for Various γ Values When $N = 64$, $\Delta t = 0.01$ and $v \in [0, 1]$ for Example 12.

	$e_\infty(h, \Delta t)$			$e_2(h, \Delta t)$		
t	$\gamma = 0.1$	$\gamma = 0.2$	$\gamma = 0.3$	$\gamma = 0.1$	$\gamma = 0.2$	$\gamma = 0.3$
0.2	2.31281×10^{-10}	3.68650×10^{-9}	1.87269×10^{-8}	1.69456×10^{-10}	2.70135×10^{-9}	1.37254×10^{-8}
0.4	2.41132×10^{-10}	3.96647×10^{-9}	2.13709×10^{-8}	1.76668×10^{-10}	2.90608×10^{-9}	1.56598×10^{-8}
0.6	2.57047×10^{-10}	4.40948×10^{-9}	2.54827×10^{-8}	1.88314×10^{-10}	3.23030×10^{-9}	1.86701×10^{-8}
0.8	2.78889×10^{-10}	5.00732×10^{-9}	3.09262×10^{-8}	2.04304×10^{-10}	3.66797×10^{-9}	2.26564×10^{-8}
1.0	3.06537×10^{-10}	5.75181×10^{-9}	3.75631×10^{-8}	2.24549×10^{-10}	4.21307×10^{-9}	2.75167×10^{-8}

Table 9 Maximum Relative Error Comparison at Different Time Stages with $\gamma = 0.5$ for Example 12.

t	FDM[47]	Proposed Method
0.5	2.61714×10^{-8}	2.80767×10^{-7}
1.0	2.07059×10^{-7}	4.63313×10^{-7}
2.0	6.11440×10^{-7}	8.69958×10^{-7}
3.0	9.47515×10^{-7}	1.32111×10^{-6}
4.0	6.87512×10^{-6}	1.51711×10^{-6}

Table 10 $e_\infty(h, \Delta t)$ at Various Time Levels Where $h = 0.02$, $\Delta t = 0.01$ and $\gamma = 0.5$ for Example 12.

t	0.5	1.0	2.0	3.0	4.0
$e_\infty(h, \Delta t)$	4.06645×10^{-7}	8.38773×10^{-7}	1.63396×10^{-6}	1.46569×10^{-6}	3.15290×10^{-7}

Table 11 $e_\infty(h, \Delta t)$ at Various Time Levels Where $h = 0.01$, $\Delta t = 0.01$ and $\gamma = 0.5$ of Example 12.

t	0.5	1.0	2.0	3.0	4.0
$e_\infty(h, \Delta t)$	2.39962×10^{-7}	6.64741×10^{-7}	1.45188×10^{-6}	1.28013×10^{-6}	1.28242×10^{-7}

Table 12 Convergence Order for Example 12 in Temporal Direction Where $h = \frac{1}{100}$ and $\gamma = 0.5$.

	FDM[47]		Proposed Method		
Δt	$e_\infty(h, \Delta t)$	Order	$e_\infty(h, \Delta t)$	$e_2(h, \Delta t)$	Order
$\frac{1}{10}$	6.03850×10^{-5}	$\cdots$	1.08453×10^{-4}	7.96216×10^{-5}	$\cdots$
$\frac{1}{20}$	1.49327×10^{-5}	2.01572	2.70761×10^{-5}	1.98783×10^{-5}	2.00198
$\frac{1}{40}$	3.55985×10^{-6}	2.06859	6.72270×10^{-6}	4.93577×10^{-6}	2.00991
$\frac{1}{80}$	7.15987×10^{-7}	2.31381	1.63378×10^{-6}	1.19972×10^{-6}	2.04083

Table 13 Convergence Order for Example 12 in Spatial Direction Where $\Delta t = \frac{1}{100}$ and $\gamma = 0.5$.

	FDM[47]		Proposed Method		
h	$e_\infty(h, \Delta t)$	Order	$e_\infty(h, \Delta t)$	$e_2(h, \Delta t)$	Order
$\frac{1}{4}$	3.55335×10^{-5}	$\cdots$	3.79958×10^{-5}	2.76733×10^{-5}	$\cdots$
$\frac{1}{8}$	8.44998×10^{-6}	2.07216	8.68896×10^{-6}	6.33612×10^{-6}	2.12858
$\frac{1}{16}$	1.65880×10^{-6}	2.34881	1.35826×10^{-6}	9.86688×10^{-7}	2.67742
$\frac{1}{32}$	3.53690×10^{-7}	2.22958	4.74662×10^{-7}	3.51171×10^{-7}	1.51679

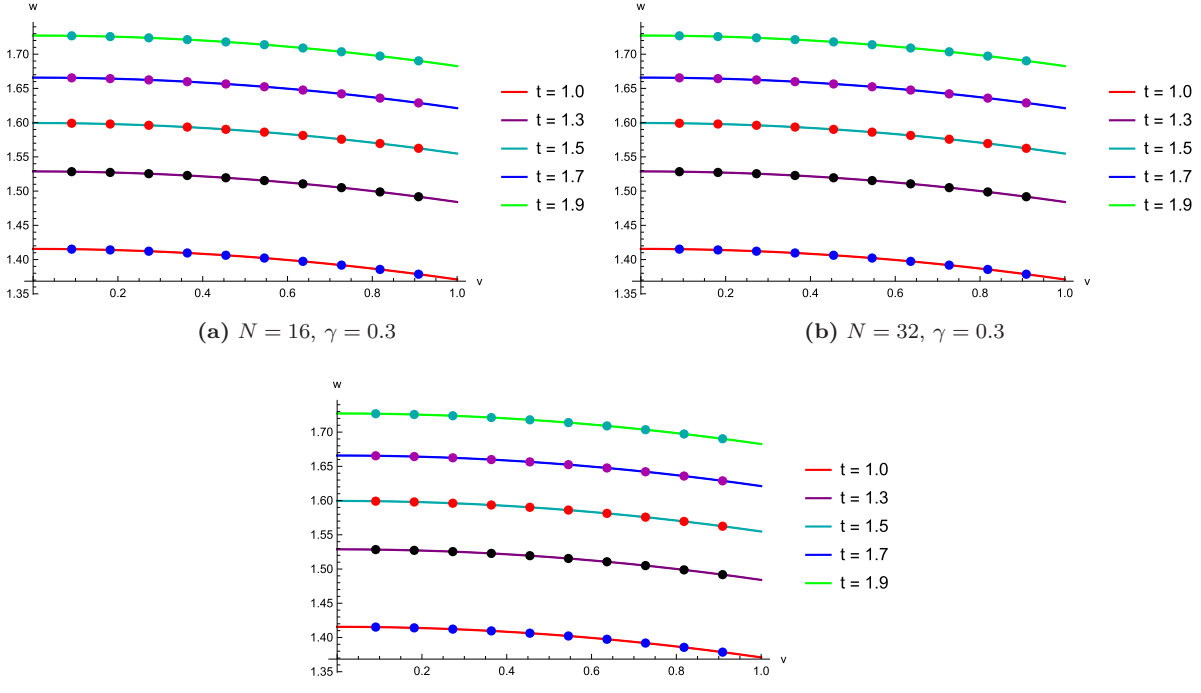

(a) $N = 16$, $\gamma = 0.3$

(b) $N = 32$, $\gamma = 0.3$

(c) $N = 16$, $\gamma = 0.5$

Fig. 5 Exact and approximate solutions at different time levels using $\Delta t = 0.01$ for Example 12.

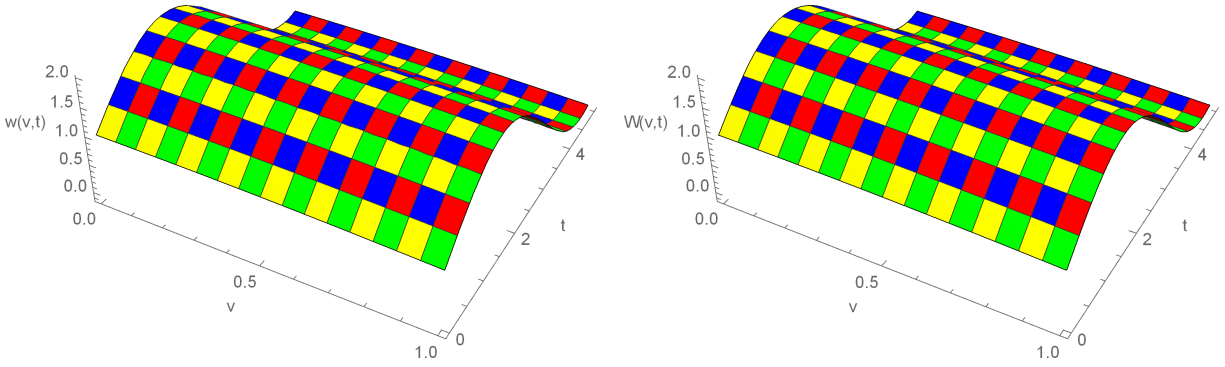

(a) Exact Solution **(b)** Approximate Solution

Fig. 6 3D exact and approximate solutions when $N = 32$, $\Delta t = 0.01$, $\gamma = 0.5$, $t = 5$ and $v \in [0, 1]$ for Example 12. and

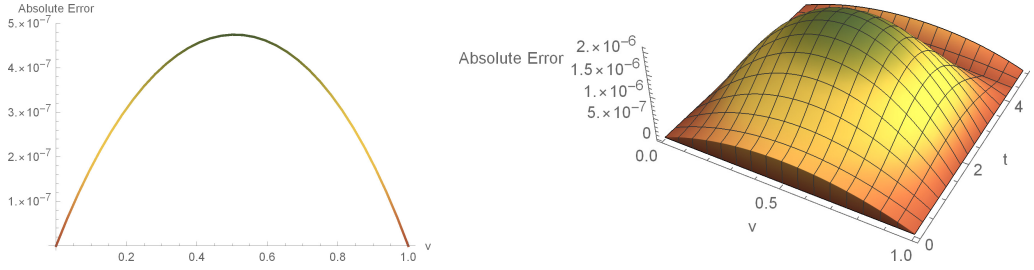

(a) 2D Error Function **(b)** 3D Error Function

Fig. 7 2D and 3D error profiles when $N = 32$, $\Delta t = 0.01$, $\gamma = 0.5$, $t = 5$ and $v \in [0, 1]$ for Example 12.

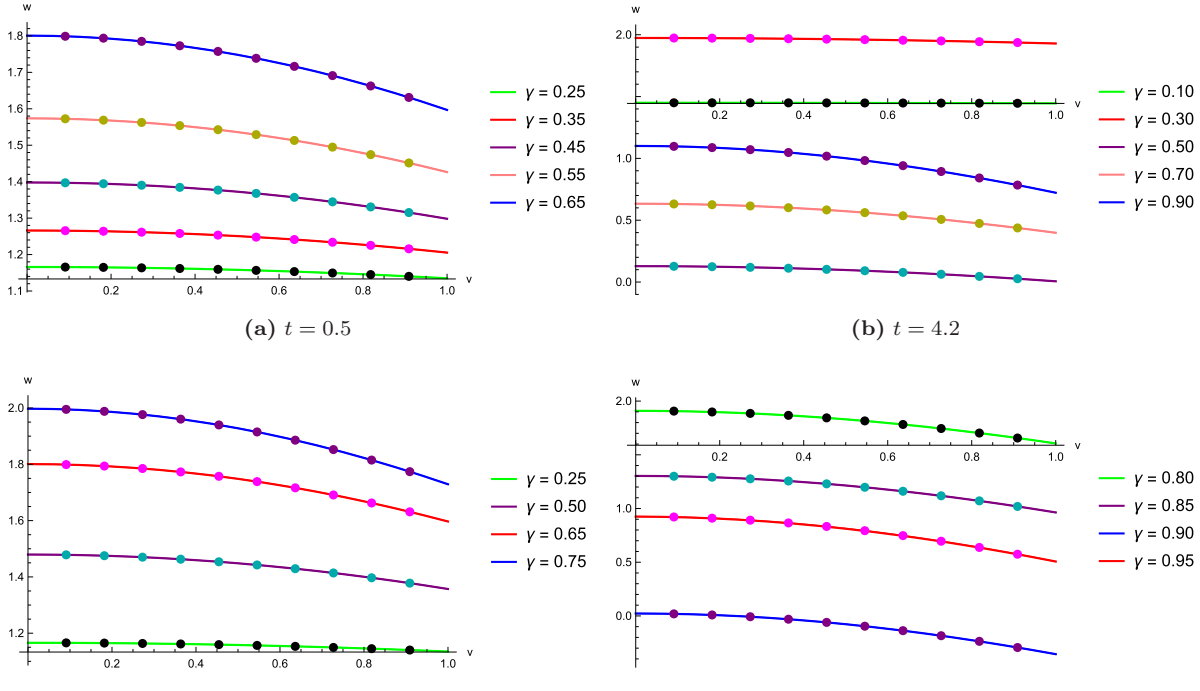

(a) $t = 0.5$ **(b)** $t = 4.2$

(c) $t = 0.5$ **(d)** $t = 0.5$

Fig. 8 Exact and approximate solutions at different γ values with $\Delta t = 0.01$ and $N = 16$ for Example 12.

with initial and end conditions

$$w(v,0) = 1 + e^v$$

and

$$w(0,t) = 1 + e^{\frac{\gamma}{1-\gamma}t}, \quad w(1,t) = e + e^{\frac{\gamma}{1-\gamma}t},$$

where $q(v,t) = \frac{1}{1-\gamma}\sinh(\frac{\gamma}{1-\gamma}t) - e^v$.

The exact solution is $w(v,t) = e^v + e^{\frac{\gamma}{1-\gamma}t}$. The absolute errors for various values of v setting $\Delta t = 0.01$, $N = 80, 100$, $\gamma = 0.5, 0.3$ and $t = 1$ are reported in Tables 14 and 15 of Example 13. In Table 16, error norms are displayed for $N = 64$, $\Delta t = 0.01$, $\gamma = 0.6$ and $v \in [0,1]$ at numerous time levels. Tables 17 and 18 expound the convergence order comparison with those reported in Ref. 47 in temporal and spatial directions, respectively. Figure 9 displays the comparison of computational solution with exact results for Example 13 at various temporal grid points by setting $\gamma = 0.3, 0.5$ and $N = 32$. A space-time plot of computational and exact results is shown in Fig. 10 for $N = 90$, $\Delta t = 0.01$, $\gamma = 0.5$ and $t = 1$. At $t = 1$, 2D and 3D error profiles are exhibited in Fig. 11. Figure 12 displays approximate and exact solutions when $\Delta t = 0.01$, $N = 16$ and $t = 1$ corresponding to various choices of γ. The numerical solutions using CBS approximations when $\gamma = 0.6, 0.5$, $0 \le v \le 1$, $t = 0.5, 1$, $h = 0.05, 0.02$ and $\Delta t = 0.01$ are given by

$$W(v,0.5) = \begin{cases} 3.117 + v(0.999883 + (0.499981 + 0.170882v)v) & \text{if } v \in [0.00, 0.05) \\ 3.117 + v(0.999948 + (0.498666 + 0.179646v)v) & \text{if } v \in [0.05, 0.10) \\ 3.11699 + v(1.00022 + (0.495902 + 0.188859v)v) & \text{if } v \in [0.10, 0.15) \\ 3.11696 + v(1.00088 + (0.491544 + 0.198545v)v) & \text{if } v \in [0.15, 0.20) \\ 3.11688 + v(1.0021 + (0.485434 + 0.208727v)v) & \text{if } v \in [0.20, 0.25) \\ 3.11671 + v(1.00411 + (0.477406 + 0.219432v)v) & \text{if } v \in [0.25, 0.30) \\ 3.1164 + v(1.00715 + (0.467278 + 0.230685v)v) & \text{if } v \in [0.30, 0.35) \\ 3.1159 + v(1.01149 + (0.454856 + 0.242515v)v) & \text{if } v \in [0.35, 0.40) \\ 3.1151 + v(1.01746 + (0.439932 + 0.254952v)v) & \text{if } v \in [0.40, 0.45) \\ 3.11391 + v(1.02541 + (0.422282 + 0.268026v)v) & \text{if } v \in [0.45, 0.50) \\ 3.11219 + v(1.03571 + (0.401664 + 0.281771v)v) & \text{if } v \in [0.50, 0.55) \\ 3.10979 + v(1.04883 + (0.377823 + 0.296221v)v) & \text{if } v \in [0.55, 0.60) \\ 3.10651 + v(1.06523 + (0.35048 + 0.311411v)v) & \text{if } v \in [0.60, 0.65) \\ 3.10212 + v(1.08547 + (0.319339 + 0.32738v)v) & \text{if } v \in [0.65, 0.70) \\ 3.09636 + v(1.11015 + (0.284084 + 0.344169v)v) & \text{if } v \in [0.70, 0.75) \\ 3.08892 + v(1.13994 + (0.244374 + 0.361818v)v) & \text{if } v \in [0.75, 0.80) \\ 3.07942 + v(1.17556 + (0.199845 + 0.380371v)v) & \text{if } v \in [0.80, 0.85) \\ 3.06744 + v(1.21784 + (0.150106 + 0.399877v)v) & \text{if } v \in [0.85, 0.90) \\ 3.05249 + v(1.26766 + (0.0947418 + 0.420382v)v) & \text{if } v \in [0.90, 0.95) \\ 3.03401 + v(1.32603 + (0.033305 + 0.441939v)v) & \text{if } v \in [0.95, 1.00) \end{cases} \tag{44}$$

Table 14 Absolute Error at Different Spatial Grid Points When $t = 1$, $N = 80$, $\gamma = 0.5$ and $\Delta t = 0.01$ of Example 13.

v	Exact Solution	Approximate Solution	Absolute Error
0.1	3.8234527465346930	3.8234527299243420	1.66104×10^{-8}
0.2	3.9396845866192150	3.9396845055345895	8.10846×10^{-8}
0.3	4.0681406360350480	4.0681404604812540	1.75554×10^{-7}
0.4	4.2101065261003150	4.2101062443559040	2.81744×10^{-7}
0.5	4.3670030991591740	4.3670027185348540	3.80624×10^{-7}
0.6	4.5404006288495540	4.5404001768060080	4.52044×10^{-7}
0.7	4.7320345359295220	4.7320340615631350	4.74366×10^{-7}
0.8	4.9438227569515130	4.9438223328607940	4.24091×10^{-7}
0.9	5.1778849396159945	5.1778846641651580	2.75451×10^{-7}

and

$$W(v,1) = \begin{cases} 3.71828 + v(0.999987 + (0.49999 + 0.168344v)v) & \text{if } v \in [0.00, 0.02) \\ 3.71828 + v(0.999991 + (0.499786 + 0.171744v)v) & \text{if } v \in [0.02, 0.04) \\ 3.71828 + v(1.00001 + (0.49937 + 0.175214v)v) & \text{if } v \in [0.04, 0.06) \\ 3.71828 + v(1.00005 + (0.498733 + 0.178753v)v) & \text{if } v \in [0.06, 0.08) \\ 3.71828 + v(1.00011 + (0.497866 + 0.182364v)v) & \text{if } v \in [0.08, 0.10) \\ 3.71828 + v(1.00023 + (0.496761 + 0.186049v)v) & \text{if } v \in [0.10, 0.12) \\ 3.71827 + v(1.00039 + (0.495408 + 0.189807v)v) & \text{if } v \in [0.12, 0.14) \\ 3.71826 + v(1.00061 + (0.493797 + 0.193641v)v) & \text{if } v \in [0.14, 0.16) \\ \quad \vdots & \\ 3.71532 + v(1.02469 + (0.424022 + 0.26667v)v) & \text{if } v \in [0.46, 0.48) \\ 3.71472 + v(1.02841 + (0.416264 + 0.272057v)v) & \text{if } v \in [0.48, 0.50) \\ 3.71403 + v(1.03253 + (0.40802 + 0.277553v)v) & \text{if } v \in [0.50, 0.52) \\ 3.71324 + v(1.03708 + (0.399273 + 0.28316v)v) & \text{if } v \in [0.52, 0.54) \\ \quad \vdots & \\ 3.67497 + v(1.19609 + (0.175502 + 0.389949v)v) & \text{if } v \in [0.84, 0.86) \\ 3.66996 + v(1.21357 + (0.155178 + 0.397826v)v) & \text{if } v \in [0.86, 0.88) \\ 3.66448 + v(1.23224 + (0.133961 + 0.405863v)v) & \text{if } v \in [0.88, 0.90) \\ 3.65851 + v(1.25217 + (0.111823 + 0.414062v)v) & \text{if } v \in [0.90, 0.92) \\ 3.65199 + v(1.27341 + (0.0887367 + 0.422427v)v) & \text{if } v \in [0.92, 0.94) \\ 3.6449 + v(1.29603 + (0.0646717 + 0.430961v)v) & \text{if } v \in [0.94, 0.96) \\ 3.6372 + v(1.3201 + (0.0395983 + 0.439667v)v) & \text{if } v \in [0.96, 0.98) \\ 3.62884 + v(1.34569 + (0.0134853 + 0.448549v)v) & \text{if } v \in [0.98, 1.00). \end{cases} \tag{45}$$

Table 15 Absolute Error at Different Spatial Grid Points When $t = 1$, $N = 100$, $\gamma = 0.3$ and $\Delta t = 0.01$ of Example 13.

v	Exact Solution	Approximate Solution	Absolute Error
0.1	2.6402339273308577	2.6402334591110255	4.68220×10^{-7}
0.2	2.7564657674153796	2.7564649092297193	8.58186×10^{-7}
0.3	2.8849218168312127	2.8849206530242460	1.16381×10^{-6}
0.4	3.0268877068964803	3.0268863296990793	1.37720×10^{-6}
0.5	3.1837842799553380	3.1837827914642450	1.48849×10^{-6}
0.6	3.3571818096457187	3.3571803240160594	1.48563×10^{-6}
0.7	3.5488157167256860	3.5488143626082764	1.35412×10^{-6}
0.8	3.7606039377476774	3.7606028610063826	1.07674×10^{-6}
0.9	3.9946661204121600	3.9946654871604155	6.33252×10^{-7}

Table 16 Error Norms When $\Delta t = 0.01$, $\gamma = 0.6$ and $N = 64$ for Example 13.

t	$e_\infty(h, \Delta t)$	$e_2(h, \Delta t)$
0.2	2.17531×10^{-6}	1.57694×10^{-6}
0.4	7.57620×10^{-7}	4.94835×10^{-7}
0.6	1.34273×10^{-6}	9.40009×10^{-7}
0.8	3.69810×10^{-6}	2.69277×10^{-6}
1.0	6.83135×10^{-6}	4.99905×10^{-6}

Table 17 Convergence Order for Example 13 in Temporal Direction Where $h = \frac{1}{100}$ and $\gamma = 0.5$.

	FDM[47]		Proposed Method		
Δt	$e_\infty(h, \Delta t)$	Order	$e_\infty(h, \Delta t)$	$e_2(h, \Delta t)$	Order
$\frac{1}{10}$	2.21374×10^{-4}	$\cdots$	2.13309×10^{-4}	1.56383×10^{-4}	$\cdots$
$\frac{1}{20}$	5.02385×10^{-5}	2.13962	5.21507×10^{-5}	3.82320×10^{-5}	2.03219
$\frac{1}{40}$	1.24729×10^{-5}	2.07000	1.18261×10^{-5}	8.66785×10^{-6}	2.14071
$\frac{1}{80}$	2.92960×10^{-6}	2.09002	1.75263×10^{-6}	1.27695×10^{-6}	2.75438

Table 18 Convergence Order for Example 13 in Spatial Direction Where $\Delta t = \frac{1}{100}$ and $\gamma = 0.5$.

	FDM[47]		Proposed method		
h	$e_\infty(h, \Delta t)$	Order	$e_\infty(h, \Delta t)$	$e_2(h, \Delta t)$	Order
$\frac{1}{4}$	9.88048×10^{-4}	$\cdots$	1.01779×10^{-3}	7.47137×10^{-4}	$\cdots$
$\frac{1}{8}$	2.48469×10^{-4}	1.99152	2.51478×10^{-4}	1.85053×10^{-4}	2.01694
$\frac{1}{16}$	2.66470×10^{-5}	1.98000	6.16166×10^{-5}	4.50280×10^{-5}	2.02904
$\frac{1}{32}$	1.57142×10^{-5}	1.99000	1.38100×10^{-5}	1.00735×10^{-5}	2.15761

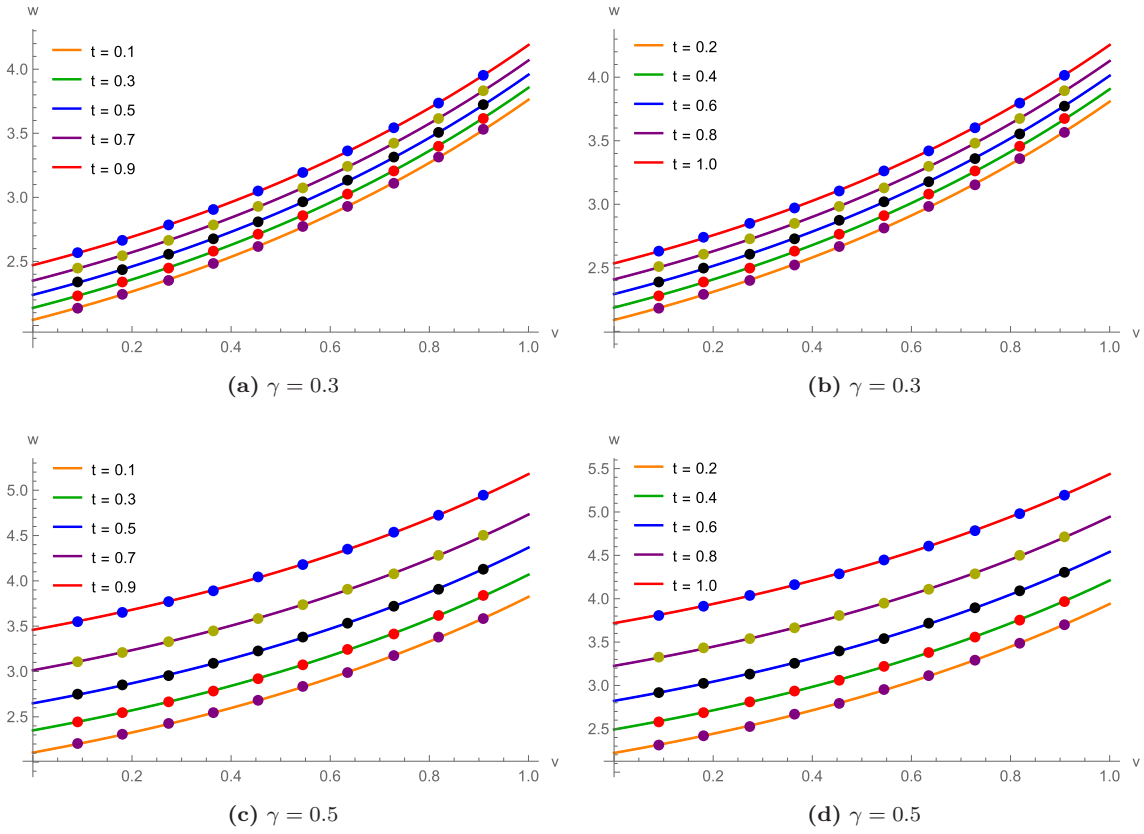

(a) $\gamma = 0.3$ **(b)** $\gamma = 0.3$

(c) $\gamma = 0.5$ **(d)** $\gamma = 0.5$

Fig. 9 Exact and approximate solutions at various time stages with $\Delta t = 0.01$ and $N = 32$ for Example 13.

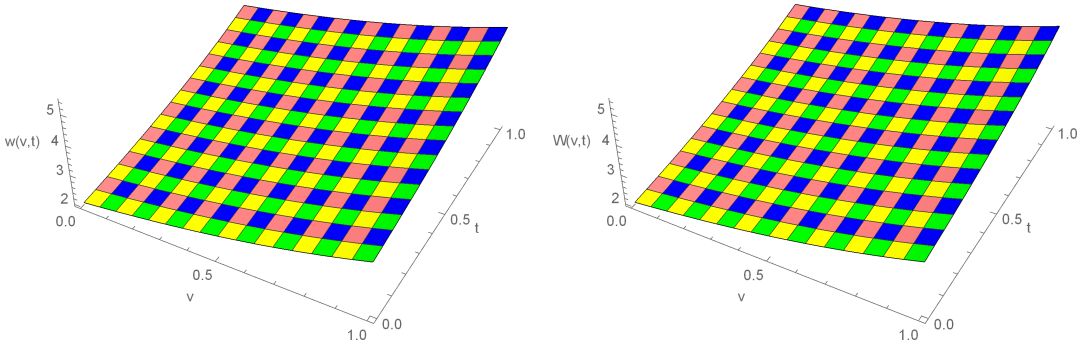

(a) Exact Solution **(b)** Approximate Solution

Fig. 10 3D exact and approximate solutions when $N = 90$, $\gamma = 0.5$, $t = 1$, $\Delta t = 0.01$ and $v \in [0, 1]$ for Example 13.

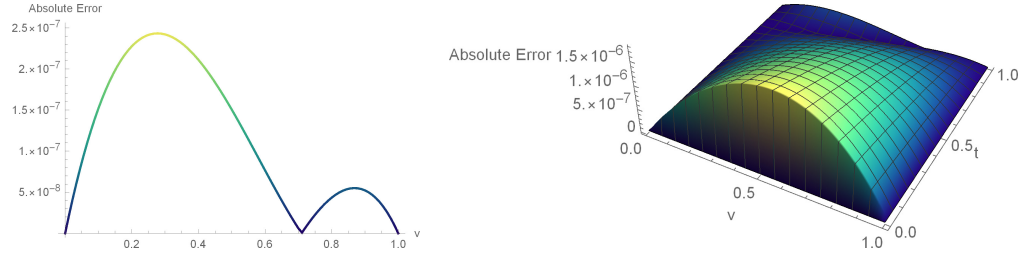

(a) 2D Error Function **(b)** 3D Error Function

Fig. 11 2D and 3D error profiles when $N = 90$, $t = 1$, $\gamma = 0.5$, $\Delta t = 0.01$ and $v \in [0, 1]$ for Example 13.

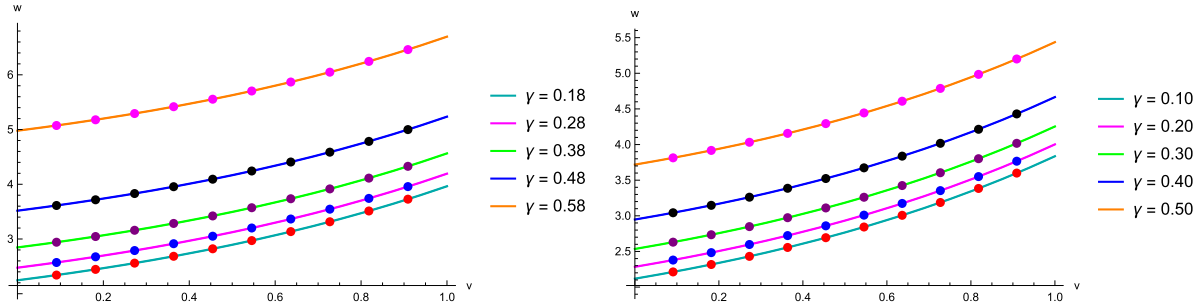

Fig. 12 Exact and approximate solutions at different γ values when $\Delta t = 0.01$, $N = 16$ and $t = 1$ of Example 13.

7. CONCLUSION

In this paper, an efficient numerical scheme based on CBS functions has been presented for solving TFDE involving Caputo–Fabrizio fractional time derivative. The non-integer order time derivative is approximated through the standard finite difference formulation while CBS functions are used to interpolate the solution curve in spatial direction. The current numerical algorithm is shown to be unconditionally stable and has second-order spatial and temporal convergence. The approximate results reveal that the presented method is reliable enough and efficient to be employed for solving mathematical models involving time fractional derivatives in Caputo–Fabrizio sense.

ACKNOWLEDGMENTS

The second author thanks to Division of Research and Innovation, Universiti Sains Malaysia for providing Article Processing Charges. The Research of fourth author was supported by Taif University Researchers Supporting Project Number (TURSP-2020/303), Taif University, Taif, Saudi Arabia. The authors are also grateful to anonymous referees for their valuable suggestions, which significantly improved this paper.

REFERENCES

1. M. Caputo and C. Cametti, Diffusion with memory in two cases of biological interest, *J. Theor. Biol.* **254**(3) (2008) 697–703.
2. M. Caputo and M. Fabrizio, Damage and fatigue described by a fractional derivative model, *J. Comput. Phys.* **293** (2015) 400–408.
3. R. L. Magin, *Fractional Calculus in Bioengineering* (Begell House Redding, 2006).
4. I. Podlubny, *Fractional Differential Equations*: *An Introduction to Fractional Derivatives*, *Fractional Differential Equations*, *to Methods of Their Solution and Some of Their Applications*, Vol. 198 (Elsevier, 1998).
5. F. Liu, V. Anh, I. Turner and P. Zhuang, Time fractional advection-dispersion equation, *J. Appl. Math. Comput.* **13**(1–2) (2003) 233–245.
6. W. R. Schneider and W. Wyss, Fractional diffusion and wave equations, *J. Math. Phys.* **30** (1989) 134–144.
7. M. M. Meerschaert and C. Tadjeran, Finite difference approximations for fractional advection-dispersion flow equations, *J. Comput. Appl. Math.* **172**(1) (2004) 65–77.
8. M. M. Meerschaert and E. Scalas, Coupled continuous time random walks in finance, *Physica A*: *Stat. Mech. Appl.* **370**(1) (2006) 114–118.
9. J. T. Machado, V. Kiryakova and F. Mainardi, Recent history of fractional calculus, *Commun. Nonlinear Sci. Numer. Simul.* **16**(3) (2011) 1140–1153.
10. R. C. Koeller, Applications of fractional calculus to the theory of viscoelasticity, *J. Appl. Mech.* **51**(2) (1984) 299–307.
11. T. S. Aleroev, H. T. Aleroeva, J. Huang, N. Nie, Y. Tang and S. Zhang, Features of seepage of a liquid to a chink in the cracked deformable layer, *Int. J. Model. Simul. Sci. Comput.* **1**(3) (2010) 333–347.
12. Y. Li, F. Liu, I. W. Turner and T. Li, Time-fractional diffusion equation for signal smoothing, *Appl. Math. Comput.* **326** (2018) 108–116.
13. K. S. Miller and B. Ross, *An Introduction to the Fractional Calculus and Fractional Differential Equations* (Wiley-Interscience, 1993).
14. S. G. Samko, A. A. Kilbas and O. I. Marichev, *Fractional Integrals and Derivative*, *Theory and Applications* (Gordon and Breach Science, 1993).
15. K. B. Oldham and J. Spanier, *The Fractional Calculus* (Academic Press, Waltham, MA, USA, 1974).
16. A. A. Kilbas, H. M. Srivastava and J. J. Trujillo, *Theory and Applications of Fractional Differential*

Equations, North-Holland Mathematics Studies, Vol. 204 (Elsevier Science, 2006).
17. A. Atangana and A. Secer, A note on fractional order derivatives and table of fractional derivatives of some special functions, in *Abstract and Applied Analysis*, Vol. 2013 (Hindawi, 2013).
18. E. C. De Oliveira and J. A. Tenreiro Machado, A review of definitions for fractional derivatives and integral, in *Mathematical Problems in Engineering*, Vol. 2014 (Hindawi, 2014).
19. P. Zhuang and F. Liu, Implicit difference approximation for the time fractional diffusion equation, *J. Appl. Math. Comput.* **22**(3) (2006) 87–99.
20. J. Q. Murillo and S. B. Yuste, An explicit difference method for solving fractional diffusion and diffusion-wave equations in the Caputo form, *J. Comput. Nonlinear Dyn.* **6**(2) (2011) 021014.
21. N. H. Sweilam, M. M. Khader and A. M. S. Mahdy, Crank–Nicolson finite difference method for solving time-fractional diffusion equation, *J. Fraction. Calc. Appl.* **2**(2) (2012) 1–9.
22. H. Sun, W. Chen and K. Y. Sze, A semi-discrete finite element method for a class of time-fractional diffusion equations, *Philos. Trans. Roy. Soc. A: Math. Phys. Eng. Sci.* **371** (1990) (2013) 20120268.
23. K. Mustapha, B. Abdallah and K. M. Furati, A discontinuous Petrov–Galerkin method for time-fractional diffusion equations, *SIAM J. Numer. Anal.* **52**(5) (2014) 2512–2529.
24. S. Esmaeili and R. Garrappa, A pseudo-spectral scheme for the approximate solution of a time-fractional diffusion equation, *Int. J. Comput. Math.* **92**(5) (2015) 980–994.
25. N. H. Tuan, L. V. C. Hoan and S. Tatar, An inverse problem for an inhomogeneous time-fractional diffusion equation: A regularization method and error estimate, *Comput. Appl. Math.* **38**(2) (2019) 32.
26. A. Atangana and B. S. T. Alkahtani, Extension of the resistance, inductance, capacitance electrical circuit to fractional derivative without singular kernel, *Adv. Mech. Eng.* **7**(6) (2015) 1–6.
27. A. Atangana and S. İ. Araz, New concept in calculus: Piecewise differential and integral operators, *Chaos Solitons Fractals* **145** (2021) 110638.
28. A. Atangana and R. T. Alqahtani, Numerical approximation of the space-time Caputo–Fabrizio fractional derivative and application to groundwater pollution equation, *Adv. Difference Equations* **2016**(1) (2016) 156.
29. N. Al-Salti, E. Karimov and K. Sadarangani, On a differential equation with Caputo–Fabrizio fractional derivative of order $1 < \beta \leq 2$ and application to mass-spring-damper system, *Fract. Different. Appl.* **2**(4) (2016) 257–263.
30. E. F. D. Goufo, Application of the Caputo–Fabrizio fractional derivative without singular kernel to Korteweg–de Vries–Burgers equation, *Math. Model. Anal.* **21**(2) (2016) 188–198.
31. I. A. Mirza and D. Vieru, Fundamental solutions to advection-diffusion equation with time-fractional Caputo–Fabrizio derivative, *Comput. Math. Appl.* **73**(1) (2017) 1–10.
32. H. Liu, A. Cheng, H. Yan, Z. Liu and H. Wang, A fast compact finite difference method for quasi–linear time fractional parabolic equation without singular kernel, *Int. J. Comput. Math.* **96**(7) (2019) 1444–1460.
33. D. Kumar, J. Singh and D. Baleanu, Modified Kawahara equation within a fractional derivative with non-singular kernel, *Thermal Sci.* **22**(2) (2018) 789–796.
34. A. Shaikh, A. Tassaddiq, K. S. Nisar and D. Baleanu, Analysis of differential equations involving Caputo–Fabrizio fractional operator and its applications to reaction-diffusion equations, *Adv. Difference Equations* **2019**(1) (2019) 178.
35. M. Yaseen, M. Abbas, A. I. Ismail and T. Nazir, A cubic trigonometric B-spline collocation approach for the fractional sub-diffusion equations, *Appl. Math. Comput.* **293** (2017) 311–319.
36. M. Yaseen, M. Abbas, T. Nazir and D. Baleanu, A finite difference scheme based on cubic trigonometric B-splines for a time fractional diffusion-wave equation, *Adv. Difference Equations* **2017**(1) (2017) 274.
37. M. Yaseen and M. Abbas, An efficient computational technique based on cubic trigonometric B-splines for time fractional burgers' equation, *Int. J. Comput. Math.* **97**(3) (2020) 725–738.
38. N. Khalid, M. Abbas, M. K. Iqbal and D. Baleanu, A numerical algorithm based on modified extended B-spline functions for solving time-fractional diffusion wave equation involving reaction and damping terms, *Adv. Difference Equations* **2019**(1) (2019) 378.
39. S. T. Mohyud-Din, T. Akram, M. Abbas, A. I. Ismail and N. H. Ali, A fully implicit finite difference scheme based on extended cubic B-splines for time fractional advection-diffusion equation, *Adv. Difference Equations* **2018**(1) (2018) 109.
40. T. Akram, M. Abbas, A. I. Ismail, N. H. M. Ali and D. Baleanu, Extended cubic B-splines in the numerical solution of time fractional telegraph equation, *Adv. Difference Equations* **2019**(1) (2019) 365.
41. N. Khalid, M. Abbas and M. K. Iqbal, Non-polynomial quintic spline for solving fourth-order fractional boundary value problems involving product terms, *Appl. Math. Comput.* **349** (2019) 393–407.
42. M. Amin, M. Abbas, M. K. Iqbal and D. Baleanu, Non-polynomial quintic spline for numerical solution of fourth-order time fractional partial differential

equations, *Adv. Difference Equations* **2019**(1) (2019) 183.
43. M. Amin, M. Abbas, M. K. Iqbal, A. I. M. Ismail and D. Baleanu, A fourth order non-polynomial quintic spline collocation technique for solving time fractional superdiffusion equations, *Adv. Difference Equations* **2019**(1) (2019) 514.
44. M. Caputo and M. Fabrizio, A new definition of fractional derivative without singular kernel, *Prog. Fraction. Different. Appl.* **1**(2) (2015) 73–85.
45. J. R. Poulin, Calculating infinite series using parseval's identity (Master Thesis), The University of Maine, Orono, ME 04469, USA (2020).
46. M. Shafiq, M. Abbas, K. M. Abualnaja, M. J. Huntul, A. Majeed and T. Nazir, An efficient technique based on cubic B-spline functions for solving time-fractional advection diffusion equation involving Atangana–Baleanu derivative, *Eng. Comput.* **38**(1) (2022) 901–917.
47. A. Taghavi, A. Babaei and A. Mohammadpour, On the stable implicit finite differences approximation of diffusion equation with the time fractional derivative without singular kernel, *Asian-Eur. J. Math.* **13**(6) (2020) 2050111.
48. W. E. Boyce, R. C. DiPrima and D. B. Meade, *Elementary Differential Equations and Boundary Value Problems*, Vol. 9 (Wiley, New York, 1992).
49. M. K. Kadalbajoo and P. Arora, B-spline collocation method for the singular-perturbation problem using artificial viscosity, *Comput. Math. Appl.* **57**(4) (2009) 650–663.
50. C. de Boor, On the convergence of odd-degree spline interpolation, *J. Approx. Theory* **1**(4) (1968) 452–463.
51. C. A. Hall, On error bounds for spline interpolation, *J. Approx. theory* **1**(2) (1968) 209–218.